arXiv:1611.06690v2 [math.PR] 12 Dec 2016

Limit distributions for KPZ growth models with spatially homogeneous random initial conditions

S. Chhita* P.L. Ferrari† H. Spohn‡

November 21, 2016

Abstract

For stationary KPZ growth in $1+1$ dimensions the height fluctuations are governed by the Baik-Rains distribution. Using the totally asymmetric single step growth model, alias TASEP, we investigate height fluctuations for a general class of spatially homogeneous random initial conditions. We prove that for TASEP there is a one-parameter family of limit distributions, labeled by the roughness of the initial conditions. The distributions are defined through a variational formula. We use Monte Carlo simulations to obtain their numerical plots. Also discussed is the connection to the six-vertex model at is conical point.

1 Introduction

For stochastic growth models in the Kardar-Parisi-Zhang (KPZ) universality class over a one-dimensional substrate the height fluctuations "always" broaden as $t^{1/3}$. On the other hand the full probability density function depends on the choice of the initial data. As well known, for a flat initial surface, $h(x, t = 0) = 0$, the large t fluctuations of $h(0, t)$ are distributed according to GOE Tracy-Widom distribution [8, 41, 53]. In contrast, if the height profile is macroscopically curved, then GOE has to be replaced by GUE [2, 4, 11, 27, 34, 46, 52]. Such dependence is not so easily inferred directly from the growth dynamics. But if one switches to the equivalent model of a directed polymer in a space-time random potential, then one end point of the polymer is fixed, while the constraints for the other end point depend on the initial conditions. For example, in the curved case the other end

*Department of Mathematical Sciences, Durham University, Stockton Road, Durham, DH1 3LE, UK. E-mail: sunil.chhita@durham.ac.uk

†Institute for Applied Mathematics, Bonn University, Endenicher Allee 60, 53115 Bonn, Germany. E-mail: ferrari@uni-bonn.de

‡Zentrum Mathematik, TU München, Boltzmannstrasse 3, D-85747 Garching, Germany. E-mail: spohn@ma.tum.de

point is fixed and in the flat case the other end point is sampled along a straight line. The size of the polymer free energy fluctuations is robust, but the probability density is sensitive to the particular end point sampling.

In our contribution we study such dependence on initial conditions in the case when the local slopes are statistically translation invariant. Besides flat, the only other known explicit example refers to initial heights which fluctuate as two-sided Brownian motion. If as a surface growth model we consider the one-dimensional KPZ equation,

$$\partial_t h = \tfrac{1}{2}(\partial_x h)^2 + \tfrac{1}{2}\partial_x^2 h + \xi \tag{1.1}$$

with $\xi(x,t)$ normalized space-time white noise, then the time-stationary initial data are

$$h(x,0) = B(x) \tag{1.2}$$

with $B(x)$ a two-sided Brownian motion. As shown in [10] (for other models in the KPZ class, see [1, 7, 26, 32]),

$$h(0,t) \simeq -\tfrac{1}{24}t + (t/2)^{1/3}\xi_{\mathrm{BR}} \tag{1.3}$$

for large t and the random amplitude ξ_{BR} is Baik-Rains distributed [7]. Recently, Quastel and Remenik [44] identified a large domain of attraction for the GOE Tracy-Widom distribution. Roughly speaking, an initial profile, $h(x,0)$, which grows slower than $|x|^{1/2}$ for large $|x|$ exhibits height fluctuations which are GOE Tracy-Widom distributed. Our interests are translation invariant random initial data, for which height differences typically grow as $|x|^{1/2}$. This is physically a rather natural assumption, since it is realized by initial slopes being approximately independent. In fact, we will exclusively focus on the one-sided growing single-step model, *alias* TASEP, with initial slope (= particle) configuration $\eta_j(t=0) = \eta_j$ taking values $0, 1$. The restriction to translation invariant initial slopes means that $\{\eta_j | j \in \mathbb{Z}\}$ is a stationary stochastic process satisfying the functional central limit theorem

$$\lim_{\ell\to\infty} \frac{2}{\sqrt{\ell}} \sum_{j=0}^{[\gamma x \ell]} \big(\eta_j - \langle\eta_0\rangle\big) = \sigma B(x) \tag{1.4}$$

for some $\sigma \geq 0$. Here γ is a scaling constant set such that $\sigma = 1$ corresponds to stationary initial conditions. As to be shown, if $\sigma = 0$, then the height fluctuations are GOE Tracy-Widom distributed, thereby strengthening the results of [44]. In our contribution we will argue, and prove under additional assumptions, that for translation invariant random initial data the universality classes are labeled by σ. For each σ there is a distinct distribution function $F^{(\sigma)}(s)$. Let us denote by ρ the expected density of particles and by j the expected (infinitesimal) current of particles. Time correlations are significant only close to the ray $\{j = \mathsf{j}'(\rho)t\}$. Thus if $\mathsf{j}'(\rho) = 0$, the height fluctuations close to the origin, as obtained from $\eta_j(t)$, are governed by $F^{(\sigma)}(s)$ in the large t limit. In case $\mathsf{j}'(\rho) \neq 0$, $F^{(\sigma)}(s)$ will be observed after properly centering (see e.g. [26] in the case $\sigma = 1$).

In Section 2 we prove that the limiting distribution is determined through a variational formula,

$$F^{(\sigma)}(s) = \mathbb{P}\Big(\sup_{x\in\mathbb{R}} \{\sqrt{2}\sigma B(x) + \mathcal{A}_2(x) - x^2\} \le s \Big), \tag{1.5}$$

where $\mathcal{A}_2(x)$ is the Airy process and is independent of the two-sided Brownian motion $B(x)$. The proof is written using the last passage percolation picture. It uses several non-trivial results obtained only recently, the most important ones being tightness [16] for the point-to-point process with ending points on horizontal lines, and the one-point slow-decorrelation [20]. Finally one also needs to know the convergence of the finite-dimensional distributions [14]. These ingredients can be used to obtain a functional slow-decorrelation result (Theorem 2.11), see [22] for the discrete time counterpart. Interestingly, this latter result then implies tightness of the point-to-point process along generic lines, see e.g. Corollary 2.13, which is a result not covered by the elegant and soft arguments of [16].

As already proved in [35], $F^{(0)}(s) = F_{\mathrm{GOE}}(2^{2/3}s)$, with F_{GOE} the GOE Tracy-Widom distribution. Our result indirectly implies that $F^{(1)}(s)$ equals the Baik-Rains distribution. The only other explicit solution corresponds formally to the limit $\sigma \to \infty$, which reads (after scaling s with $\sigma^{4/3}$, see also Section 3.1)

$$\mathbb{P}\Big(\sup_{x\in\mathbb{R}} \{B(x) - x^2\} \le s \Big). \tag{1.6}$$

An explicit representation is provided in [30]. Its probability density vanishes for $s < 0$ and decays as a stretched exponential with power $\frac{3}{2}$ for $s \to \infty$.

For all other values of σ we have to rely on Monte Carlo simulations, which will be reported in Section 3. A convenient choice is to simulate the TASEP dynamics and to independently sample η_j as a reversible Markov chain. The average density is taken as $\frac{1}{2}$ and varying the only remaining parameter one can achieve $0 \le \sigma < \infty$. To check the claimed universality we also simulate the diagonal transfer matrix of the six-vertex model at its stochastic point, see Section 4. For the equilibrium Gibbs measure of this model, the Baik-Rains distribution has been proved recently [1].

Acknowledgments. The authors are grateful for discussions with Ivan Corwin and Kazumasa Takeuchi. This work started when two of us visited in early 2016 the Kavli Institute of Theoretical Physics at Santa Barbara. The work of P.L. Ferrari and S. Chhita is supported by the German Research Foundation as part of the SFB 1060–B04 project.

2 Convergence to the variational formula

In this section we prove the variational formula (1.5) for the totally asymmetric simple exclusion process (TASEP) in continuous time, which is directly related to the last passage percolation (LPP) model with exponential waiting times. Thus we first recall the models and their well known relation.

2.1 TASEP and LPP

Let us first recall the relation between TASEP and LPP. A last passage percolation (LPP) model on $\mathbb{Z}^2$ with independent random variables $\{\omega_{i,j}, i,j \in \mathbb{Z}\}$ is the following. An *up-right path* $\pi = (\pi(0), \pi(1), \ldots, \pi(n))$ on $\mathbb{Z}^2$ from a point A to a point E is a sequence of points in $\mathbb{Z}^2$ with $\pi(k+1) - \pi(k) \in \{(0,1),(1,0)\}$, with $\pi(0) = A$ and $\pi(n) = E$, and where n is called the length $\ell(\pi)$ of π. Now, given a set of points S_A and E, one defines the last passage time $L_{S_A \to E}$ as

$$L_{S_A \to E} = \max_{\substack{\pi: A \to E \\ A \in S_A}} \sum_{1 \le k \le \ell(\pi)} \omega_{\pi(k)}. \tag{2.1}$$

Finally, we denote by $\pi^{\max}_{S_A \to E}$ any maximizer of the last passage time $L_{S_A \to E}$. For continuous random variables, the maximizer is a.s. unique.

TASEP is an interacting particle system on $\mathbb{Z}$ with state space $\Omega = \{0,1\}^{\mathbb{Z}}$. Here η is the occupation variable, which is 1 at site j if and only if j is occupied by a particle. TASEP has generator L given by [40]

$$Lf(\eta) = \sum_{j \in \mathbb{Z}} \eta_j (1 - \eta_{j+1}) \big(f(\eta^{j,j+1}) - f(\eta) \big), \tag{2.2}$$

where f are local functions (depending only on finitely many sites) and $\eta^{j,j+1}$ denotes the configuration η with the occupations at sites j and $j+1$ interchanged. Notice that for the TASEP the ordering of particles is preserved. That is, if initially one orders from right to left as

$$\ldots < x_2(0) < x_1(0) < 0 \le x_0(0) < x_{-1}(0) < \cdots,$$

then for all times $t \ge 0$ also $x_{n+1}(t) < x_n(t)$, $n \in \mathbb{Z}$.

Concerning the mapping between TASEP and LPP, the $\omega_{i,j}$ in the LPP is the waiting time of particle j to jump from site $i-j-1$ to site $i-j$. By definition $\omega_{i,j}$ are exp(1) iid. random variables. Let $S_A = \{(u,k) \in \mathbb{Z}^2 : u = k + x_k(0), k \in \mathbb{Z}\}$. Then, the relationship between TASEP and LPP is given by

$$\mathbb{P}\left(L_{S_A \to (m,n)} \le t\right) = \mathbb{P}\left(x_n(t) \ge m - n\right). \tag{2.3}$$

Further, for $m = n$,

$$\mathbb{P}\left(L_{S_A \to (n,n)} \le t\right) = \mathbb{P}\left(x_n(t) \ge 0\right) = \mathbb{P}\left(J(t) \ge n\right), \tag{2.4}$$

where $J(t)$ counts the number of jumps from site 0 to site 1 during the time-span $[0,t]$.

To state the variational problem for TASEP, we have to first reformulate the TASEP as a growth process by introducing the height function $h(j,t)$ which is defined by

$$h(j,t) = \begin{cases} 2J(t) + \sum_{i=1}^{j} (1 - 2\eta_i(t)) & \text{for } j \ge 1, \\ 2J(t) & \text{for } j = 0, \\ 2J(t) - \sum_{i=j+1}^{0} (1 - 2\eta_i(t)) & \text{for } j \le -1, \end{cases} \tag{2.5}$$

for $j \in \mathbb{Z}$, $t \geq 0$.

The well-studied cases corresponding to $\sigma = 0$, resp. $\sigma = 1$, in (1.5), are obtained by choosing periodic initial conditions ($x_j(0) = -2j, j \in \mathbb{Z}$), resp. stationary initial conditions [39] ($\eta_i(0)$, $i \in \mathbb{Z}$, are taken to be i.i.d. Bernoulli-ρ random variables, $\rho \in (0,1)$). In this work we consider for simplicity $\rho = 1/2$ because in this case the characteristic lines for the associated PDE (Burgers equation) corresponds to the space-time lines with fixed spatial coordinate. Considering other densities does not require any additional technical difficulty, as one introduces appropriate space-shifts, which only slightly complicates the formulas. Here is the assumption on the initial condition.

Assumption 2.1. *The height function $j \mapsto h(j,0)$ weakly converges under a Brownian scaling to a two-sided Brownian motion with drift 0 and diffusion constant σ^2. Explicitly,*

$$x \mapsto \frac{h([\gamma \ell x], 0)}{\sqrt{\ell}} \to \sigma B(x) \quad \text{as } \ell \to \infty, \tag{2.6}$$

where B is a standard two-sided Brownian motion. Here γ is a model-dependent scaling constant fixed by the property that $\sigma = 1$ is the stationary case.

Theorem 2.2. *Let us define the distribution function*

$$F^{(\sigma)}(s) := \mathbb{P}\left(\max_{u \in \mathbb{R}} \left[\sqrt{2}\sigma B(u) + \big(\mathcal{A}_2(u) - u^2\big) \right] \leq s \right). \tag{2.7}$$

Then, under Assumption 2.1, for any $s \in \mathbb{R}$ it holds

$$\lim_{t \to \infty} \mathbb{P}\left(h(0,t) \geq t/2 - s(t/2)^{1/3} \right) = F^{(\sigma)}(s). \tag{2.8}$$

Remark 2.3. As opposed to considering the reference point $x = 0$, choose instead the reference point $x = 2\xi(t/2)^{2/3}$, which then leads to

$$\begin{aligned} \lim_{t \to \infty} \mathbb{P}\left(h(2\xi(t/2)^{2/3}, t) \geq t/2 - s(t/2)^{1/3} \right) \\ = \mathbb{P}\left(\max_{u \in \mathbb{R}} \left[\sqrt{2}\sigma B(u) + \big(\mathcal{A}_2(u) - (u-\xi)^2\big) \right] \leq s \right). \end{aligned} \tag{2.9}$$

Note that the transition function from flat to stationary is in the parameter σ and differs from the flat to stationary transition that can be found e.g. in (1.27) of [44] or in (56) of [22], as this is a transition with respect to the reference point. For fixed σ, the process in ξ has only been characterized for $\sigma = 0$ (the Airy_1 process [12, 45]) and $\sigma = 1$ (the $\mathrm{Airy}_{\mathrm{stat}}$ process [5]).

For the simulation part, the initial condition which satisfies Assumption 2.1 is obtained using the following Markov chain: $\{\eta_j(0), j \in \mathbb{Z}\}$ is a stationary Markov chain with transition matrix

$$T = \begin{pmatrix} \alpha & 1-\alpha \\ 1-\alpha & \alpha \end{pmatrix}. \tag{2.10}$$

The stationary one-point distribution is $\mathbb{P}(\eta_j = 0) = \mathbb{P}(\eta_j = 1) = 1/2$.

Lemma 2.4. *The height function obtained through the stationary Markov chain with transition matrix T satisfies Assumption 2.1 with $\gamma = 1$ and $\sigma^2 = \alpha/(1-\alpha)$.*

This result can be obtained in various ways. One can use the coupling contained in the proof of Theorem 1 of [47] between a Brownian motion and the correlated random walk, which replaces the standard Skorokhod embedding in the proof of Donsker's theorem for the convergence of random walks to Brownian motions. Another option is to consider the two last increment of the height function as the state of the system and then one recovers the Markov property. Using the fact that the height function is then a linear functional of the Markov process one recovers the result by using Kipnis-Varadhan Theorem [37].

Remark 2.5. Corwin, Liu and Wang consider discrete time TASEP with parallel updates and q being the probability of not jumping. They obtain an analogue variational formula with $\sigma = q^{-1/4} \in (1, \infty)$, see (53) in [22], where the initial condition is product Bernoulli. To consider the full range of σ, one need to consider families of random initial condition as we do in our paper.

Remark 2.6. One could drop the assumption of translation-invariance for the initial height profile, such that the limit on the right side of (2.6) will be another non-degenerate limit process, say $\mathcal{R}$. As soon as the condition (2.15) in the proof is satisfied for $\mathcal{R}$ instead of σB, then Theorem 2.2 will also hold, where of course $\sqrt{2}\sigma B(u)$ is replaced by $\sqrt{2}\mathcal{R}(u)$.

2.2 Proof of Theorem 2.2

The key ingredients to prove Theorem 2.2 are (a) functional slow-decorrelation, (b) bounds that ensures that the optimizer stays within a specific region. Due to Lemma 2.4, we know that the random line for the discrete model converges weakly to a Brownian motion as a continuous function. Therefore we know that if we restrict the maximization problem to a region of width $M\ell^{2/3}$ around the origin, the random line will typically deviate from the anti-diagonal of order $\sqrt{M}\ell^{1/3}$. We will prove a functional slow-decorrelation which says that the fluctuations of the LPP problem from the anti-diagonal and those lines at distance $\mathcal{O}(\ell^\nu)$ away from it with $\nu < 1$, do not exceed $\varepsilon\ell^{1/3}$ for any $\varepsilon > 0$, in the $\ell \to \infty$ limit. This gives control of the LPP from the random line, when restricted to a $M\ell^{2/3}$-neighborhood of the origin. Finally, we show that the probability that the maximizer starts more than $M\ell^{1/3}$ away from the origin tends to zero as M tends to infinity (we get a bound in M which goes to zero and which is uniform in ℓ).

One main difference between our proof and the one of the case of geometric random variables of [22], is that we do not use the Gibbs property of the associated multilayer model to bound the probability of LPP from small segments through point-to-point probabilities, rather we bound this probability directly using the fact that the kernel for the half-line problem is known. This simplifies the approach for the estimates of the moderate/large deviations made in [22]. To prove

the functional slow-decorrelation theorem we need a tightness result, which for exponential random variables was recently obtained by Cator and Pimentel with an elegant argument [16]. Interestingly, the functional slow-decorrelation allows to deduce tightness on other space-time cuts, where the soft-argument do not directly apply.

Proof of Theorem 2.2. The randomness from the initial conditions and the randomness from the dynamics provide two independent sources of randomness in the system. From the LPP perspective, these two sources become the randomness in the line from which the last passage time is taken and the randomness of the weights $\omega_{i,j}$'s respectively. As the LPP only allows up-right paths, these must be contained inside the set $\mathcal{B}_\ell = \{(m,n) \in \mathbb{R}^2 \,|\, m,n \le \frac{1}{4}\ell\}$. *All the sets that defined below are to be thought to be subsets of $\mathcal{B}_\ell$, but for notational simplicity, this is suppressed.* For instance, here we write $\mathcal{L} = \{(k + x_k(0), k), k \in \mathbb{Z}\}$ instead of the same set intersected with $\mathcal{B}_\ell$. Set $t = \ell + 2^{2/3}\ell^{1/3}s$, which means that $\ell = t - 2^{2/3}t^{1/3}s + o(t^{-1/3})$, and (2.4) gives

$$\begin{aligned}\mathbb{P}(h(0,t) \ge t/2 - s(t/2)^{1/3}) &= \mathbb{P}(J(t) \ge \tfrac{1}{4}t - s2^{-4/3}t^{1/3}) \\ &= \mathbb{P}(L_{\mathcal{L}\to(\frac{1}{4}t - s2^{-4/3}t^{1/3}, \frac{1}{4}t - s2^{-4/3}t^{1/3})} \le t) \\ &= \mathbb{P}(L_{\mathcal{L}\to(\ell/4,\ell/4)} \le \ell + 2^{2/3}\ell^{1/3}s) = \mathbb{P}(E_{\mathcal{L},\ell,s}),\end{aligned} \tag{2.11}$$

where we define the event

$$E_{\mathcal{L},\ell,s} = \{L_{\mathcal{L}\to(\ell/4,\ell/4)} \le \ell + 2^{2/3}\ell^{1/3}s\}. \tag{2.12}$$

For any given $M \ge 1$, we define the domains

$$\mathcal{D}_{M,\ell} = \{(m,n) \in \mathbb{R}^2 \,|\, |m+n| \le (\ell/2)^{2/3}, |m-n| \le M(\ell/2)^{2/3}\}, \tag{2.13}$$

and $\mathcal{C}_{M,\ell} = \mathcal{C}^+_{M,\ell} \cup \mathcal{C}^-_{M,\ell}$, where

$$\mathcal{C}^-_{M,\ell} = \bigcup_{k=1}^{\varepsilon_0\ell^{1/3}} \{(m,n) \in \mathbb{R}^2 \,|\, n \ge kM(\ell/2)^{2/3}, m+n \ge -\tfrac{1}{4}k^2M^2(\ell/2)^{1/3}\} \tag{2.14}$$

is the region on the right of $\mathcal{L}^-_{M,\ell}$, and $\mathcal{C}^+_{M,\ell}$ is the mirror image of $\mathcal{C}^-_{M,\ell}$ with respect to the axis $\{m = n\}$; see Figure 1. For a standard two-sided Brownian motion B,

$$\lim_{M\to\infty}\lim_{\ell\to\infty} \mathbb{P}(\{(\tfrac{1}{2}(x + \sigma B(x)), \tfrac{1}{2}(\sigma B(x) - x)), x \in \mathbb{R}\} \subset \mathcal{D}_{M,\ell} \cup \mathcal{C}_{M,\ell}) = 1. \tag{2.15}$$

This, together with the weak convergence of $\mathcal{L}$ to σB (rotated by 45), see Lemma 2.4 below, implies that

$$\lim_{M\to\infty}\lim_{\ell\to\infty} \mathbb{P}(\mathcal{L} \subset \mathcal{D}_{M,\ell} \cup \mathcal{C}_{M,\ell}) = 1, \tag{2.16}$$

and consequently

$$\lim_{M\to\infty}\lim_{\ell\to\infty} \mathbb{P}(E_{\mathcal{L},\ell,s}) = \mathbb{P}(E_{\mathcal{L},\ell,s} | \mathcal{L} \subset \mathcal{D}_{M,\ell} \cup \mathcal{C}_{M,\ell}). \tag{2.17}$$

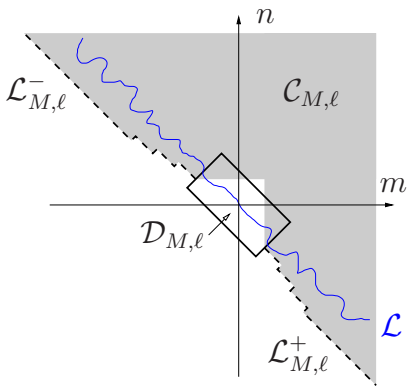

Figure 1: Illustration of the main lines and domains used in the proof. The domain $\mathcal{C}_{M,\ell}$ is the gray one, while $\mathcal{D}_{M,\ell}$ is the rectangular region. The thick dashed lines are $\mathcal{L}^{\pm}_{M,\ell}$.

For notational simplicity, let us denote by $\mathbb{P}_M(\cdot) = \mathbb{P}(\cdot|\mathcal{L} \subset \mathcal{D}_{M,\ell} \cup \mathcal{C}_{M,\ell})$.

By definition of the LPP time, $L_{\mathcal{L}\to(\ell/4,\ell/4)} = \max_{I\in\mathcal{L}} L_{I\to(\ell/4,\ell/4)}$. The maximum is obtained a.s. at a unique point (as the random waiting times have densities). Notice that $E_{\mathcal{L},\ell,s}$ holds if and only if both $E_{\mathcal{L}\cap\mathcal{D}_M,\ell,s}$ and $E_{\mathcal{L}\cap\mathcal{C}_M,\ell,s}$ hold. Theorem 2.7 below implies that for any given $M \geq M_0$ (with M_0 a constant)

$$\mathbb{P}_M(E_{\mathcal{L}\cap\mathcal{C}_M,\ell,s})) \geq 1 - Ce^{-cM} \tag{2.18}$$

uniformly for $\ell \geq \ell_0$, where C and c are constants independent of ℓ. Therefore

$$\lim_{M\to\infty}\lim_{\ell\to\infty} \mathbb{P}_M(E_{\mathcal{L},\ell,s}) = \lim_{M\to\infty}\lim_{\ell\to\infty} \mathbb{P}_M(E_{\mathcal{L}\cap\mathcal{D}_M,\ell,s}). \tag{2.19}$$

For a given I, we denote by I_0 its orthogonal projection on the line $\{(m,n) \in \mathbb{R}^2 \,|\, m+n=0\}$, that is, the anti-diagonal. We now introduce the following coordinates: $I_0 = I_0(u) = u(\ell/2)^{2/3}(-1,1)$ and for this I_0, we denote by $I = I(u)$ the point on $\mathcal{L}$ connected by a line of slope 1; see Figure 2. With these notations we can write

$$\begin{aligned} E_{\mathcal{L}\cap\mathcal{D}_M,\ell,s} &= \{\max_{|u|\leq M} L_{I(u)\to(\ell/4,\ell/4)} \leq \ell + 2^{2/3}\ell^{1/3}s\} \\ &= \{\max_{|u|\leq M} L_{I_0(u)\to(\ell/4,\ell/4)} + (L_{I(u)\to(\ell/4,\ell/4)} - L_{I_0(u)\to(\ell/4,\ell/4)}) \leq \ell + 2^{2/3}\ell^{1/3}s\}. \end{aligned} \tag{2.20}$$

Now we use the functional slow-decorrelation theorem, given in Theorem 2.11 below: for any $\varepsilon > 0$, the good event

$$G_{\mathcal{L},M,\ell,\varepsilon} = \{\max_{|u|\leq M} |L_{I(u)\to(\ell/4,\ell/4)} - L_{I_0(u)\to(\ell/4,\ell/4)} - 4m(I(u)) + 4m(I_0(u))| \leq 2^{2/3}\ell^{1/3}\varepsilon\} \tag{2.21}$$

occurs with probability 1 as $\ell \to \infty$. Therefore for any $\varepsilon > 0$

$$(2.19) = \lim_{M\to\infty}\lim_{\ell\to\infty} \mathbb{P}_M(E_{\mathcal{L}\cap\mathcal{D}_M,\ell,s} \cap G_{\mathcal{L},M,\ell,\varepsilon}). \tag{2.22}$$

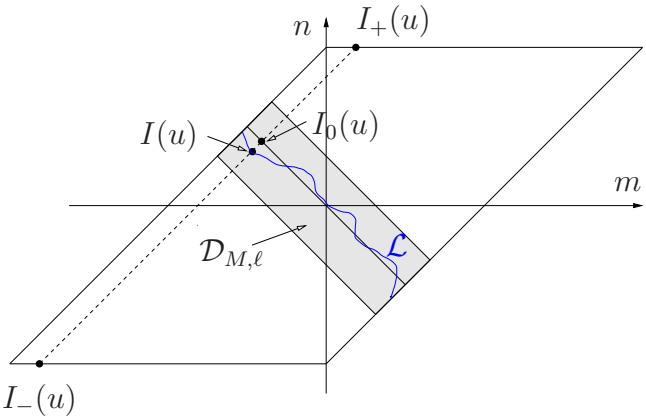

Figure 2: LPP with random initial condition $\mathcal{L}$.

Further,

$$\begin{aligned}
&\mathbb{P}_M(E_{\mathcal{L}\cap\mathcal{D}_M,\ell,s}\cap G_{\mathcal{L},M,\ell,\varepsilon})\\
&=\mathbb{P}_M(\{\max_{|u|\le M} L_{I(u)\to(\ell/4,\ell/4)}\le \ell+2^{2/3}\ell^{1/3}s\}\cap G_{\mathcal{L},M,\ell,\varepsilon})\\
&\le \mathbb{P}\Big(\{\max_{|u|\le M}\frac{L_{I_0(u)\to(\ell/4,\ell/4)}-\ell+4m(I(u))-4m(I_0(u))}{2^{2/3}\ell^{1/3}}\le s+\varepsilon\}\cap G_{\mathcal{L},M,\ell,\varepsilon}\Big).
\end{aligned}\tag{2.23}$$

A lower bound to $\mathbb{P}_M(E_{\mathcal{L}\cap\mathcal{D}_M,\ell,s}\cap G_{\mathcal{L},M,\ell,\varepsilon})$ is obtained by replacing ε by $-\varepsilon$ in the same way. By Lemma 2.4, $\mathcal{L}$ converges weakly to a Brownian motion path with diffusivity constant σ^2 as $\ell\to\infty$, i.e., to σB. An elementary calculation gives

$$\lim_{\ell\to\infty}\frac{4m(I(u))-4m(I_0(u))}{2^{2/3}\ell^{1/3}}=\sqrt{2}\sigma B(u).\tag{2.24}$$

Further, $\frac{L_{I_0(u)\to(\ell/4,\ell/4)}-\ell}{2^{2/3}\ell^{1/3}}$ as a stochastic process in $u\in[M,M]$ converges weakly to $\mathcal{A}_2(u)-u^2$ (with $\mathcal{A}_2$ being the Airy$_2$ process [36, 43]), see Corollary 2.13 (alternatively, one could consider I to be the projection to the m-axis directly, with the only difference that the difference of the LPP from $I(u)$ and from $I_0(u)$ is now a Brownian motion with a drift, exactly compensating the linear term in (2.56)). Thus

$$\begin{aligned}
\lim_{M\to\infty}\lim_{\ell\to\infty}(2.23)&=\lim_{M\to\infty}\mathbb{P}\Big(\max_{|u|\le M}\Big[\mathcal{A}_2(u)-u^2+\sqrt{2}\sigma B(u)\Big]\le s+\varepsilon\Big)\\
&=\mathbb{P}\Big(\max_{u\in\mathbb{R}}\Big[\mathcal{A}_2(u)-u^2+\sqrt{2}\sigma B(u)\Big]\le s+\varepsilon\Big),
\end{aligned}\tag{2.25}$$

where the last equality is due to the fact that distributions of the positions of the maximum of $\mathcal{A}_2(u)-u^2/2$ and $\sqrt{2}\sigma B(u)-u^2/2$ are tight (for the Airy$_2$ case, see Proposition 4.4 of [21] or Proposition 2.13 in [22], while for the Brownian motion it is obvious as we can control it with a Brownian motion with a drift away from the origin; see [29–31] for explicit formulas). This, together with the analogous lower

bound holds for any $\varepsilon > 0$. Thus we have shown the convergence in distribution in Theorem 2.2. The limiting distribution function in (2.7) is continuous as the Airy_2 process is locally Brownian (use inequalities (103)-(104) and the localizing bound (88) in [22]). □

In the next theorem we show that the LPP from $\mathcal{C}_{M,\ell}$ is typically lower than the one from the origin, from which one can prove that the maximizer is localized to occur in $\mathcal{D}_{M,\ell}$. The probability that this does not occur goes to zero as $M \to \infty$ as expected, since $\mathcal{C}_{M,\ell}$ stays on the right of the constant limit shape.

Theorem 2.7. *Let $\mathcal{C}_{M,\ell}$ defined just after (2.13) and let $\mathcal{L}_{M,\ell} = \partial\mathcal{C}_{M,\ell}$ be the boundary of it. For any fixed $s \in \mathbb{R}$, there is a $M_0 > 0$ such that for all given $M > M_0$, there exists a $\ell_0 \in (0,\infty)$ such that*

$$\mathbb{P}(L_{\mathcal{L}_{M,\ell}\to(\ell/4,\ell/4)} < \ell + 2^{2/3}\ell^{1/3}s) > 1 - Ce^{-cM} \tag{2.26}$$

uniformly for $\ell \geq \ell_0$. The constants C and c are ℓ-independent.

Proof. Denote by

$$\mathcal{L}_{kM,\ell} = \partial\{(m,n) \in \mathbb{R}^2 \,|\, n > kM(\ell/2)^{2/3}, m+n > -\tfrac{1}{4}k^2M^2(\ell/2)^{1/3}\}. \tag{2.27}$$

Symmetry and union bounds give

$$\mathbb{P}(L_{\mathcal{L}_{M,\ell}\to(\ell/4,\ell/4)} > \ell+2^{2/3}\ell^{1/3}s) \leq 2\sum_{k=1}^{\varepsilon_0\ell^{1/3}} \mathbb{P}(L_{\mathcal{L}_{kM,\ell}\to(\ell/4,\ell/4)} > \ell+2^{2/3}\ell^{1/3}s). \tag{2.28}$$

In order to study the right side of the above equation, recall the mapping between LPP and TASEP as given in (2.4). Since $\mathcal{L}_{kM,\ell} \to (\ell/4,\ell/4)$ is a half-line with slope -1 taking values in the second quadrant, this LPP corresponds to TASEP with an initial condition in which particles occupy every second position below a threshold and there are no particles above the threshold. The distribution function of this TASEP is given by a Fredholm determinant with an explicit kernel derived in [13]. Namely, from [13, Proposition 3], we have the formula

$$\mathbb{P}(x_n(t) \geq a) = 1 - \det(\mathbb{1} - \chi_a K_{n,t}\chi_a)_{\ell^2(\mathbb{Z})} \tag{2.29}$$

where $\chi_a(x) = \mathbb{1}_{[x<a]}$ and

$$K_{n,t}(y_1,y_2) = \frac{1}{(2\pi\mathrm{i})^2}\oint_{\Gamma_0}\mathrm{d}v\oint_{\Gamma_{-1,-1-v}}\mathrm{d}u\frac{e^{-vt}(1+v)^{y_2+n}}{v^n}\frac{e^{ut}u^n}{(1+u)^{y_1+n+1}}\frac{1+2v}{(u-v)(1+u+v)} \tag{2.30}$$

with $-\Gamma_0 - 1$ is contained inside $\Gamma_{-1,-1-v}$. Note that this kernel is equal to zero if $y_1 \leq -2n-1$ (no residues anymore). To find the specific formula for this theorem, notice that by a translation of the LPP, the summand on the right side of (2.28) gives

$$\begin{aligned}&\mathbb{P}(L_{\mathcal{L}_{kM,\ell}\to(\ell/4,\ell/4)} > \ell + 2^{2/3}\ell^{1/3}s)\\ &= \mathbb{P}(L_{\mathcal{L}_{0,0}\to(\ell/4+(kM)(\ell/2)^{2/3}+\frac{1}{4}(kM)^2(\ell/2)^{1/3},\ell/4-(kM)(\ell/2)^{2/3})} > \ell + 2^{2/3}\ell^{1/3}s).\end{aligned} \tag{2.31}$$

Using the TASEP and LPP mapping, (2.4), we have

$$\begin{aligned}&\mathbb{P}(L_{\mathcal{L}_{0,0}\to(\ell/4+(kM)(\ell/2)^{2/3}+\frac{1}{4}(kM)^2(\ell/2)^{1/3},\ell/4-(kM)(\ell/2)^{2/3})} > \ell + 2^{2/3}\ell^{1/3}s)\\ &= \mathbb{P}(x_{\ell/4-(kM)(\ell/2)^{2/3}}(\ell + 2^{2/3}\ell^{1/3}s) < 2(kM)(\ell/2)^{2/3} + \tfrac{1}{4}(k^2M^2)(\ell/2)^{1/3}).\end{aligned} \tag{2.32}$$

The above equation indicates the scalings

$$\begin{aligned}t &= \ell + 2^{2/3}\ell^{1/3}s\\ n &= \ell/4 - (kM)(\ell/2)^{2/3}\\ y_i &= 2(kM)(\ell/2)^{2/3} + \tfrac{1}{4}(k^2M^2)(\ell/2)^{1/3} - 2(\ell/2)^{1/3}\xi_i.\end{aligned} \tag{2.33}$$

with $\xi_1, \xi_2 \in [0, \infty)$, where the latter condition is from the indicator function in (2.29). We define the rescaled and conjugated kernel to be

$$K^{\mathrm{resc}}(\xi_1, \xi_2) = 2^{y_2 - y_1 + 1}\,(\ell/2)^{1/3}\,K_{n,t}(y_1, y_2) \tag{2.34}$$

with n and t given in (2.33).

To conclude the proof of the theorem, we need bounds on K^{resc}, which are given in Lemma 2.8 below. Set $a = 2(kM)(\ell/2)^{2/3} + \frac{1}{4}(k^2M^2)(\ell/2)^{1/3}$. We expand the Fredholm determinant associated to the right side of (2.32) which gives

$$\sum_{m=0}^{\infty} \frac{(-1)^m}{m!} \sum_{z_1=-\infty}^{\infty} \cdots \sum_{z_m=-\infty}^{\infty} \prod_{i=1}^{m} \chi_a(z_i) \det\left[K_{t,n}(z_i, z_j)\right]_{1\le i,j\le m}. \tag{2.35}$$

In the above formula, we set each $z_i = a - 2\xi_i(\ell/2)^{1/3}$, use the rescaled kernel and evaluate the Riemann sums to find that the above formula becomes

$$\sum_{m=0}^{\infty} \frac{(-1)^m}{m!} \int_0^{\infty} \mathrm{d}\xi_1 \ldots \int_0^{\infty} \mathrm{d}\xi_m \det\left[K^{\mathrm{resc}}(\xi_i, \xi_j)\right]_{1\le i,j\le m}. \tag{2.36}$$

Let us choose M large enough (such that $|s| < M$), then from Lemma 2.8, we factor out $e^{-c(kM)^3}e^{-\xi_i}$ from the above determinant. Using Hadamard's bound in the standard way we can conclude that (2.36) is bounded above by $Ce^{-ck^3M^3} < Ce^{-ckM}$. Therefore, the right side of (2.28) is bounded above by

$$\sum_{k=1}^{\varepsilon_0\ell^{1/3}} Ce^{-ckM} \le Ce^{-cM}(1 - e^{-cM})^{-1} \le 2Ce^{-cM} \tag{2.37}$$

for M large enough. Since the estimate found in Lemma 2.8 is uniform, the above bound is uniform in ℓ. □

Lemma 2.8. *For all $k \in \{1, \ldots, \varepsilon_0\ell^{1/3}\}$ and $|s| < M$, the estimate*

$$|K^{\mathrm{resc}}(\xi_1, \xi_2)| \le \frac{C}{(kM)^2} e^{-c_1(kM)^3 - c_2(kM)(\xi_2 + s)} \tag{2.38}$$

holds uniformly in ℓ for all $\xi_1, \xi_2 \ge 0$, where $C, c_1, c_2 > 0$ are constants.

Proof of Lemma 2.8. For convenience, set $\varepsilon = \varepsilon(k, M, \ell) = kM(\ell/2)^{-1/3}$.

The proof of this result is via a steepest descent analysis. We remark that we do not deform the contours of integration to pass through the critical points. It is more convenient to deform the contours to be relatively close to the critical point giving a less optimal estimate, but this is sufficient for our purposes.

Define

$$g_0(v) = -4v + (1 + 2\varepsilon + \varepsilon^2/2)\log 2(1+v) - (1-2\varepsilon)\log v. \tag{2.39}$$

Then, with the scalings given in (2.33), we have

$$\log\left(\frac{e^{-vt}(2(1+v))^{y_2+n}}{v^n}\right) = \frac{\ell}{4}g_0(v) - 2\left(\frac{\ell}{2}\right)^{1/3}\xi_2\log(2(1+v)) - 2\left(\frac{\ell}{2}\right)^{1/3}sv. \tag{2.40}$$

We have a similar expression for $\log(e^{-ut}u^n/(2(1+u))^{y_1+n})$.

Define $C_0 = \{v : |v| = 1/2 - \varepsilon\}$, $C_1 = \{u : |u+1| = 1/2\}$ and set $\Gamma_0 = C_0$, $\Gamma_{-1,-1-v} = C_1$. Further, set $C_0^\delta = \{v \in C_0 : |v + 1/2 - \varepsilon| < \delta\}$ and $C_1^\delta = \{u \in C_1 : |u + 1/2| < \delta\}$. Then, we can write $C_0 \cup C_1 = C_0^\delta \cup C_1^\delta + \Sigma$, where Σ is the remaining contour. Notice that for $v \in \Sigma$, $\mathrm{Re}(g_0(v) - g_0(-1/2+\varepsilon)) \le -c_3$ for some $c_3 = c_3(\delta)$ because $\mathrm{Re}(v)$ increases when moving away from $-1/2+\varepsilon$ along the contour C_0 and the same is true for $\log|1+v|$. By a similar reasoning, we have $\mathrm{Re}(g_0(u) - g_0(-1/2)) \ge c_3$. We also have for $u \in C_1$ and $v \in C_0$,

$$\left|\frac{1+2v}{(u-v)(1+u+v)}\right| \le \frac{C}{\varepsilon}. \tag{2.41}$$

Using the above bound and observations, we conclude that

$$\begin{aligned}&\left(\frac{\ell}{2}\right)^{1/3}\left|\frac{4}{(2\pi\mathrm{i})^2}\iint_\Sigma \mathrm{d}u\,\mathrm{d}v\frac{e^{-vt}(2(1+v))^{y_2+n}}{v^n}\frac{e^{ut}u^n}{(2(1+u))^{y_1+n+1}}\frac{1+2v}{(u-v)(1+u+v)}\right| \\ &\le C\frac{\ell^{1/3}}{\varepsilon}e^{-c_3\ell/2}\end{aligned} \tag{2.42}$$

for ℓ large enough. This is because the smaller terms in the exponential in ℓ are bounded by ℓc_3, which dominates the $\ell^{1/3}$ terms.

For the integral over C_k^δ's, using $|u+1| = 1/2$, we have

$$\begin{aligned}&\left|\frac{4\left(\frac{\ell}{2}\right)^{1/3}}{(2\pi\mathrm{i})^2}\int_{C_1^\delta}\mathrm{d}u\int_{C_0^\delta}\mathrm{d}v\frac{e^{-vt}(2(1+v))^{y_2+n}}{v^n}\frac{e^{ut}u^n}{(2(1+u))^{y_1+n+1}}\frac{1+2v}{(u-v)(1+u+v)}\right| \\ &\le \frac{\left(\frac{\ell}{2}\right)^{1/3}}{\pi^2}\int_{C_1^\delta}\mathrm{d}u\int_{C_0^\delta}\mathrm{d}v\left|e^{\frac{\ell}{4}(g_0(v)-g_0(u))}e^{-2\left(\frac{\ell}{2}\right)^{1/3}(\xi_2\log(2(1+v))+sv-su)}\right|\left|\frac{1+2v}{(u-v)(1+u+v)}\right|.\end{aligned} \tag{2.43}$$

Introduce $v = -\frac{1}{2} + \varepsilon + V$, $u = -\frac{1}{2} + U$, $\gamma_0^\delta = C_0^\delta - 1/2 + \varepsilon$ and $\gamma_1^\delta = C_1^\delta - 1/2$. A Taylor series expansion gives

$$\begin{aligned}g_0(u) &= g_0(-\tfrac{1}{2}) + g_0'(-\tfrac{1}{2})U + \tfrac{1}{2}g_0''(-\tfrac{1}{2})U^2 + O(U^3) \\ &= g_0(-\tfrac{1}{2}) + \varepsilon^2 U - \varepsilon(8+\varepsilon)U^2 + O(U^3)\end{aligned} \tag{2.44}$$

and

$$\begin{aligned} g_0(-\tfrac{1}{2}+\varepsilon) &= g_0(-\tfrac{1}{2}+\varepsilon) + g_0'(-\tfrac{1}{2}+\varepsilon)V + \tfrac{1}{2}g_0''(-\tfrac{1}{2}+\varepsilon)V^2 + O(V^3) \\ &= g_0(-\tfrac{1}{2}+\varepsilon) + \frac{\varepsilon^2}{1+2\varepsilon}V + \frac{2\varepsilon(\varepsilon(2\varepsilon+15)+8)}{(1-2\varepsilon)(2\varepsilon+1)^2}V^2 + O(V^3). \end{aligned} \tag{2.45}$$

Set

$$P = \exp\left[\frac{\ell}{4}\mathrm{Re}\left(g_0(-\tfrac{1}{2}+\varepsilon) - g_0(-\tfrac{1}{2})\right) - 2\left(\frac{\ell}{2}\right)^{1/3}(\xi_2\log(1+2\varepsilon)+\varepsilon s)\right] \tag{2.46}$$

which is computed later. Using the above change of variables and expansions for the right side of (2.43) gives

$$\begin{aligned} &\frac{2^2\left(\frac{\ell}{2}\right)^{1/3}P}{(2\pi)^2}\int_{\gamma_1^\delta}\mathrm{d}U\int_{\gamma_0^\delta}\mathrm{d}V\left|\frac{2\epsilon+2V}{(U+\varepsilon+V)(\varepsilon+V-U)}\right|\left|e^{O(\ell V^3,\ell U^3,\ell^{1/3}(\xi_2+s)V^2)}\right| \\ &\times\exp\left[\frac{\ell}{4}\left(\frac{\varepsilon^2}{1+2\varepsilon}V + \frac{2\varepsilon(\varepsilon(2\varepsilon+15)+8)}{(1-2\varepsilon)(2\varepsilon+1)^2}V^2 - \varepsilon^2U + \varepsilon(8+\varepsilon)U^2\right)\right]\Bigg|. \end{aligned} \tag{2.47}$$

To the above equation, we make a further change of variables

$$U = \frac{w}{\ell^{1/2}}\frac{\sqrt{2}}{\sqrt{\varepsilon(8+\varepsilon)}} \quad \text{and} \quad V = \frac{z}{\ell^{1/2}}\frac{\sqrt{1-2\varepsilon}(2\varepsilon+1)}{\sqrt{\varepsilon(\varepsilon(2\varepsilon+15)+8)}} \tag{2.48}$$

and let $\tilde{\gamma}_1^\delta$ and $\tilde{\gamma}_0^\delta$ be the images of γ_1^δ and γ_0^δ under these change of variables. These change of variables applied to (2.47) imply that (2.43) is bounded above by

$$\begin{aligned} &\frac{CP\ell^{1/3}}{\varepsilon\ell}\int_{\tilde{\gamma}_1^\delta}\mathrm{d}w\int_{\tilde{\gamma}_0^\delta}\mathrm{d}z\left|\frac{2\varepsilon+O(z\ell^{-1/2})}{\varepsilon^2+O(\varepsilon z\ell^{-1/2},\varepsilon z\ell^{-1/2})}\right|\left|e^{O(z^3\ell^{-1/2},w^3\ell^{-1/2},\ell^{-2/3}(\xi_2+s)z^2)}\right| \\ &\times\left|e^{\frac{1}{2}(w^2+z^2)}\right|\left|\exp\left[\varepsilon^2\frac{z}{\ell^{1/2}}\frac{\sqrt{1-2\varepsilon}}{\sqrt{\varepsilon(\varepsilon(2\varepsilon+15)+8)}} - \varepsilon^2\frac{w\sqrt{2}}{\ell^{1/2}\sqrt{\varepsilon(8+\varepsilon)}}\right]\right|. \end{aligned} \tag{2.49}$$

A good approximation of the contour $\tilde{\gamma}_1^\delta$ is an interval on the imaginary axis. This means that the exponential term involving z is highly oscillatory but has an absolute value equal to 1. Choose δ small enough so that $O(\ell^{-1/2}z^3) \ll z^2$, $O(\ell^{-1/2}z) \ll 1$ (and also $O(\ell^{-1/2}z) \ll O(\varepsilon)$). Furthermore, choose δ small enough suc that $M\delta^2 \ll 1$. This means that the exponential terms in the above integral with respect to z are bounded above by $|\exp(\chi_0\frac{z^2}{2})|$ with $\chi_0 > 0$. Here, χ_0 can be made close to 1, by choosing δ small enough. A similar statement can be made for the integral with respect to w. These observations to (2.49) imply that (2.43) is bounded by

$$\frac{CP\ell^{1/3}}{\varepsilon^2\ell}\int_{\tilde{\gamma}_1^\delta}\mathrm{d}z\int_{\tilde{\gamma}_0^\delta}\mathrm{d}w\left|e^{\frac{1}{2}(w^2+z^2)}\right|. \tag{2.50}$$

The contours $\tilde{\gamma}_0^\delta$ and $\tilde{\gamma}_0^\delta$ can be extended to the whole imaginary axis with no significant error, resulting in a computable Gaussian integral which is finite. Using $\varepsilon = kM(\ell/2)^{-1/3}$ we obtain

$$|(2.43)| \leq \frac{CP}{(kM)^2}. \tag{2.51}$$

It remains to compute P. We have that

$$\mathrm{Re}(g_0(-\tfrac{1}{2}+\varepsilon) - g_0(-\tfrac{1}{2})) = -4\varepsilon + (1+2\varepsilon+\tfrac{1}{2}\varepsilon^2)\log(1+2\varepsilon) - (1-2\varepsilon)\log(1-2\varepsilon). \tag{2.52}$$

Provided that ε_0 is small enough, we apply a Taylor series expansion to find that

$$\mathrm{Re}(g_0(-\tfrac{1}{2}+\varepsilon) - g_0(-\tfrac{1}{2})) = -\frac{5}{3}\varepsilon^3 + O(\varepsilon^4), \tag{2.53}$$

which means

$$\frac{\ell}{4}\mathrm{Re}(g_0(-\tfrac{1}{2}+\varepsilon) - g_0(-\tfrac{1}{2})) = -c_1(kM)^3 + O(\varepsilon_0 \ell^{-1/3}). \tag{2.54}$$

We also have

$$2\left(\frac{\ell}{2}\right)^{1/3}(\xi_2 \log(1+2\varepsilon) + \varepsilon s) = c_2 kM(\xi_2(1+O(\varepsilon_0\ell^{-1/3})) + s), \tag{2.55}$$

which means that $P \leq e^{-c_1(kM)^3 - c_2(kM)(\xi_2+s)}$ for an appropriate choice of positive constants c_1 and c_2. Substituting this bound for P into (2.51) gives the result. □

Below we prove the missing ingredients in the proof of Theorem 2.2, in particular the functional slow-decorrelation result (Theorem 2.11). This result is the analogue of Theorem 2.15 of [22] for the case of geometric random variables. In the proof one needs tightness (the analogue of Lemma 5.3 of [35] for the geometric case). Fortunately, for the case of exponential random variables, this result was obtained with soft arguments in [16].

Proposition 2.9 (Compare with Theorem 4 of [16])**.** *Consider the LPP from the horizontal line* $\{(m,n) \in \mathbb{Z}^2 \,|\, n = 0\}$*, and rescale it as*

$$L_\ell^{\mathrm{res,h}}(u) := \frac{L_{(-2u(\ell/2)^{2/3},0)\to(\ell/4,\ell/4)} - (\ell + 4u(\ell/2)^{2/3} - 2^{2/3}u^2\ell^{1/3})}{2^{2/3}\ell^{1/3}}, \tag{2.56}$$

for $u \in \mathbb{R}$ *with* $2u(\ell/2)^{2/3} \in \mathbb{Z}$ *and linearly interpolate for the other values of* u*. Then, for any given* $M > 0$*, the collection* $\{L_\ell^{\mathrm{res,h}}\}$ *is tight in the space of continuous functions of* $[-M,M]$*,* $\mathcal{C}([-M,M])$*. Furthermore,* $L_\ell^{\mathrm{res,h}}$ *as a stochastic process in* $u \in [M,M]$ *converges weakly to the Airy*$_2$ *process.*

Proof. Tightness along the horizontal line was already shown in Theorem 4 of [16] with a soft argument that uses a comparison with the stationary case. In that

paper, the statement is written in the space of càdlàg functions. However by inspecting the bounds used in the proof, one realizes that these are strong enough to get tightness in the space of continuous functions. The convergence of finite dimensional distributions for this exponential waiting times and along the horizontal line is a special case of [14], or can be obtained from the finite-dimensional distributions along other lines using slow-decorrelation [20]; see [5] for an application of this technique. These two ingredients imply weak convergence [9]. □

Remark 2.10. *For geometric random variable this statement was shown in Theorem 1.2 in [35], which is obtained by controlling the modulus of continuity (Lemma 5.3 in [35]) together with the convergence of the finite-dimensional distributions.*

We are ready to prove the functional slow-decorrelation theorem. This is the analogue of Theorem 2.15 of [22], which holds for geometric random variables, (slightly) specialized to our setting.

Theorem 2.11. *Let $\mathcal{L}$ be any down-right path in $\mathcal{D}_M$ going between the two sides with constant $m-n$. For $I_0(u) = u(\ell/2)^{2/3}(1,-1)$, let $I(u)$ be the point in $\mathcal{L}$ whose orthogonal projection along $(1,1)$ is $I_0(u)$. Denote by $\mu((\ell_1,\ell_2)) = (\sqrt{\ell_1}+\sqrt{\ell_2})^2$ to be the limit shape approximation of $L_{(0,0)\to(\ell_1,\ell_2)}$. Then consider the rescaled LPP processes from the anti-diagonal, $L^{\mathrm{res,ad}}$, and from the line $\mathcal{L}$, $L^{\mathrm{res},\mathcal{L}}$ (with linear interpolation as in Proposition 2.9). Define*

$$\begin{aligned} L_\ell^{\mathrm{res,ad}}(u) &:= \frac{L_{I_0(u)\to(\ell/4,\ell/4)} - \mu((\ell/4,\ell/4) - I_0(u))}{2^{2/3}\ell^{1/3}}, \\ L_\ell^{\mathrm{res},\mathcal{L}}(u) &:= \frac{L_{I(u)\to(\ell/4,\ell/4)} - \mu((\ell/4,\ell/4) - I(u))}{2^{2/3}\ell^{1/3}}. \end{aligned} \tag{2.57}$$

Then, $L_\ell^{\mathrm{res,ad}} - L_\ell^{\mathrm{res},\mathcal{L}}$ converges in probability to 0 in $\mathcal{C}([-M,M])$ as $\ell\to\infty$. Explicitly, there are $\varepsilon,\delta>0$ and a ℓ_0, such that for all $\ell\geq\ell_0$,

$$\mathbb{P}\Big(\max_{|u|\leq M} |L_\ell^{\mathrm{res,ad}}(u) - L_\ell^{\mathrm{res},\mathcal{L}}(u)| \geq \delta\Big) < \varepsilon. \tag{2.58}$$

In the proof, we use known results for the point-to-point LPP with exponential random variables, which we recall here.

Proposition 2.12. *For $\eta\in(0,\infty)$ define $\mu = (\sqrt{\eta\ell}+\sqrt{\ell})^2$, $\sigma = \eta^{-1/6}(1+\sqrt{\eta})^{4/3}$, and the rescaled random variable*

$$L_\ell^{\mathrm{res}} := \frac{L_{(0,0)\to(\eta\ell,\ell)} - \mu}{\sigma\ell^{1/3}}. \tag{2.59}$$

(a) Limit law

$$\lim_{\ell\to\infty} \mathbb{P}(L_\ell^{\mathrm{res}} \leq s) = F_{\mathrm{GUE}}(s), \tag{2.60}$$

with F_{GUE} the GUE Tracy-Widom distribution function.
(b) Bound on upper tail: there exists constants s_0, ℓ_0, C, c such that

$$\mathbb{P}(L_\ell^{\mathrm{res}} \geq s) \leq Ce^{-cs} \tag{2.61}$$

for all $\ell \geq \ell_0$ and $s \geq s_0$.
(c) Bound on lower tail: there exists constants s_0, ℓ_0, C, c such that

$$\mathbb{P}(L_\ell^{\mathrm{res}} \leq s) \leq Ce^{-c|s|^{3/2}} \tag{2.62}$$

for all $\ell \geq \ell_0$ and $s \leq -s_0$.

(a) was proven in Theorem 1.6 of [34]. Using the relation with the Laguerre ensemble of random matrices (Proposition 6.1 of [3]), or to TASEP described above, the distribution is given by a Fredholm determinant. An exponential decay of its kernel leads directly to (b). See e.g. Proposition 4.2 of [24] or Lemma 1 of [6] for an explicit statement. (c) was proven in [6] (Propositon 3 together with (56)). In the present language it is reported in Proposition 4.3 of [24] as well.

Proof of Theorem 2.11. The proof is similar to the one of Theorem 2.15 of [22], except that this time tightness is known on a horizontal slice of $\mathbb{Z}^2$ (see Proposition 2.9). To prove (2.58) it is enough to prove it for $L_\ell^{\mathrm{res,h}}$ instead of $L_\ell^{\mathrm{res,ad}}$. Indeed, the anti-diagonal satisfies the requirements for $\mathcal{L}$ and one uses the triangle inequality

$$|L_\ell^{\mathrm{res,ad}}(u) - L_\ell^{\mathrm{res},\mathcal{L}}(u)| \leq |L_\ell^{\mathrm{res,h}}(u) - L_\ell^{\mathrm{res,ad}}(u)| + |L_\ell^{\mathrm{res,h}}(u) - L_\ell^{\mathrm{res},\mathcal{L}}(u)|. \tag{2.63}$$

Thus we need to show

$$\mathbb{P}\Big(\max_{|u|\leq M} |L_\ell^{\mathrm{res,h}}(u) - L_\ell^{\mathrm{res},\mathcal{L}}(u)| \geq \delta \Big) < \varepsilon. \tag{2.64}$$

Let us consider two horizontal lines that 'enclose' the set $\mathcal{D}_{M,\ell}$, see Figure 2. We choose the lines parameterized by

$$I_\pm(u) = -2u(\ell/2)^{2/3}(1,0) \pm 2M(\ell/2)^{2/3}(1,1), \quad |u| \leq M, \tag{2.65}$$

and define $L_\ell^{\mathrm{res},\pm}(u)$ as in (2.57) with $I_0(u)$ replaced by $I_\pm(u)$. To prove (2.64) we use the inequalities

$$\begin{aligned} \mathbb{P}\Big(\max_{|u|\leq M} L_\ell^{\mathrm{res,h}}(u) - L_\ell^{\mathrm{res},\mathcal{L}}(u) \geq \delta \Big) &\leq \mathbb{P}\Big(\max_{|u|\leq M} L_\ell^{\mathrm{res,h}}(u) - L_\ell^{\mathrm{res},+}(u) \geq \delta/2 \Big) \\ &\quad + \mathbb{P}\Big(\max_{|u|\leq M} L_\ell^{\mathrm{res},+}(u) - L_\ell^{\mathrm{res},\mathcal{L}}(u) \geq \delta/2 \Big) \end{aligned} \tag{2.66}$$

and similarly

$$\begin{aligned} \mathbb{P}\Big(\max_{|u|\leq M} L_\ell^{\mathrm{res},\mathcal{L}}(u) - L_\ell^{\mathrm{res,h}}(u) \geq \delta \Big) &\leq \mathbb{P}\Big(\max_{|u|\leq M} L_\ell^{\mathrm{res},\mathcal{L}}(u) - L_\ell^{\mathrm{res},-}(u) \geq \delta/2 \Big) \\ &\quad + \mathbb{P}\Big(\max_{|u|\leq M} L_\ell^{\mathrm{res},-}(u) - L_\ell^{\mathrm{res,h}}(u) \geq \delta/2 \Big). \end{aligned} \tag{2.67}$$

Below we consider only (2.66) as (2.67) is threaded in a similar way. First we prove the following: for any $\varepsilon, \delta > 0$, there exists a ℓ_0 (depending on M only) such that for all $\ell \geq \ell_0$,

$$\mathbb{P}\Big(\max_{|u|\leq M} |L_\ell^{\mathrm{res},+}(u) - L_\ell^{\mathrm{res,h}}(u)| \geq \delta/2 \Big) < \varepsilon/2. \tag{2.68}$$

First of all, notice that tightness of $L_\ell^{\mathrm{res,h}}$ implies also tightness of $L_\ell^{\mathrm{res},\pm}$ as they are essentially the same process:

$$L_\ell^{\mathrm{res},+}(u) = (1 + 4M(\ell/2)^{-1/3})^{-1/3} L^{\mathrm{res,h}}_{\ell - 8M(\ell/2)^{2/3}}(u + \mathcal{O}(\ell^{-1/3})). \tag{2.69}$$

Thus, for M, ε, δ given above, there exists constants δ_1, ℓ_1 such that for all $\ell \geq \ell_1$,

$$\mathbb{P}\Big(\max_{|u_1|,|u_2|\leq M, |u_1-u_2|\leq \delta_1} |L_\ell^{\mathrm{res},*}(u_1) - L_\ell^{\mathrm{res},*}(u_2)| \geq \delta/6 \Big) < \varepsilon/6, \quad * \in \{+, \mathrm{h}\}. \tag{2.70}$$

Let us define $u_j = j\delta_1$ with $j \in \mathbb{Z}$ satisfying $u_j \in [-M, M]$. Since the number of j's is finite, from the usual slow-decorrelation result (Theorem 2.1 of [20]), there exists some constant ℓ_2 (depending on $\varepsilon, \delta, \delta_1$) such that for all $\ell \geq \ell_2$,

$$\mathbb{P}\Big(\max_{j:|u_j|\leq M} |L_\ell^{\mathrm{res},+}(u_j) - L_\ell^{\mathrm{res,h}}(u_j)| \geq \delta/6 \Big) < \varepsilon/6. \tag{2.71}$$

For a given $u \in [-M, M]$, choose a j such that $|u_j - u| \leq \delta_1$. Then,

$$\begin{aligned} |L_\ell^{\mathrm{res},+}(u) - L_\ell^{\mathrm{res,h}}(u)| \leq{}& |L_\ell^{\mathrm{res},+}(u) - L_\ell^{\mathrm{res},+}(u_j)| + |L_\ell^{\mathrm{res},+}(u_j) - L_\ell^{\mathrm{res,h}}(u_j)| \\ &+ |L_\ell^{\mathrm{res,h}}(u_j) - L_\ell^{\mathrm{res,h}}(u)|, \end{aligned} \tag{2.72}$$

which, together with (2.70) and (2.71), implies (2.68) as claimed.

Finally we prove: for any $\varepsilon, \delta > 0$, there exists a ℓ_0 (depending on M only) such that for all $\ell \geq \ell_0$,

$$\mathbb{P}\Big(\max_{|u|\leq M} L_\ell^{\mathrm{res},+}(u) - L_\ell^{\mathrm{res},\mathcal{L}}(u) \geq \delta/2 \Big) < \varepsilon/2. \tag{2.73}$$

Since the rescaled LPP are defined by linear interpolation between lattice-points, the maximum in (2.73) is effectively only on $\mathcal{O}(\ell^{2/3})$ number of points and thus it is enough to have a bound on $\mathbb{P}\Big(L_\ell^{\mathrm{res},+}(u) - L_\ell^{\mathrm{res},\mathcal{L}}(u) \geq \delta/2 \Big)$, which multiplied by $\ell^{2/3}$ goes to 0 as $\ell \to \infty$.

Without rescaling, since the maximizers from $I(u)$ to $(\ell/4, \ell/4)$ can pass by $I_+(u)$ (and will pass close to it since $I_+(u)$ is essentially on the characteristic line between $I(u)$ and $(\ell/4, \ell/4)$), we have

$$L_{I(u)\to(\ell/4,\ell/4)} \geq L_{I(u)\to I_+(u)} + L_{I_+(u)\to(\ell/4,\ell/4)}. \tag{2.74}$$

A simple algebraic computation shows that

$$\mu((\ell/4, \ell/4) - I(u)) = \mu((\ell/4, \ell/4) - I_+(u)) + \mu(I_+(u) - I(u)) + \mathcal{O}(1), \tag{2.75}$$

where the $\mathcal{O}(1)$ term is independent of ℓ (and bounded uniformly for $|u| \le M$). Thus (2.74) holds also in the rescaled version up to a correction $\mathcal{O}(\ell^{-1/3})$:

$$L_\ell^{\mathrm{res},+}(u) - L_\ell^{\mathrm{res},\mathcal{L}}(u) \le -\frac{L_{I(u)\to I_+(u)} - \mu(I_+(u) - I(u))}{2^{2/3}\ell^{1/3}} + \mathcal{O}(\ell^{-1/3}). \tag{2.76}$$

With the choice of $I_+(u)$, $I_+(u) - I(u) = \mathcal{O}(\ell^{2/3})$ and thus by Proposition 2.12 we have that $\frac{L_{I(u)\to I_+(u)} - \mu(I_+(u)-I(u))}{\sigma\ell^{2/9}}$ converges to a non-degenerate random variable. Since, however, we divide by $\ell^{1/3} \gg \ell^{2/9}$, the right side of (2.76) will converge to 0. Take ℓ large enough such that the error term $\mathcal{O}(\ell^{-1/3})$ is bounded by $\delta/4$. Then

$$\begin{aligned}\mathbb{P}\Big(L_\ell^{\mathrm{res},+}(u) - L_\ell^{\mathrm{res},\mathcal{L}}(u) \le \delta/2\Big) &\le \mathbb{P}\Big(\frac{L_{I(u)\to I_+(u)} - \mu(I_+(u) - I(u))}{2^{2/3}\ell^{1/3}} \le -\delta/4\Big)\\ &\le \mathbb{P}\Big(\frac{L_{I(u)\to I_+(u)} - \mu(I_+(u) - I(u))}{2^{2/3}\ell^{2/9}} \ge -\delta\ell^{1/9}/4\Big)\\ &\le Ce^{-c(\delta)\ell^{1/6}}\end{aligned} \tag{2.77}$$

where the last inequality comes from Proposition 2.12(c). Thus we have obtained the required bound to prove (2.73), which was the last piece in the proof of Theorem 2.11. □

Corollary 2.13. *Consider the LPP from $\{(m,n) \in \mathbb{Z}^2 \,|\, n+m = 0\}$, the anti-diagonal, and rescale it as*

$$L_\ell^{\mathrm{res,ad}}(u) := \frac{L_{(u(\ell/2)^{2/3}, -u(\ell/2)^{2/3})\to(\ell/4,\ell/4)} - (\ell - 2^{2/3}u^2\ell^{1/3})}{2^{2/3}\ell^{1/3}}, \tag{2.78}$$

for $u \in \mathbb{R}$ with $u(\ell/2)^{2/3} \in \mathbb{Z}$ and linearly interpolate for the other values of u. Then, for any given $M > 0$, the collection $\{L_\ell^{\mathrm{res}}\}$ is tight in the space of continuous functions of $[-M, M]$. Furthermore, L_ℓ^{res} as a stochastic process in $u \in [M, M]$ converges weakly to the Airy$_2$ process.

Proof. This follows from Theorem 2.9 and Theorem 2.11, since in the latter we can take $\mathcal{L}$ to be the anti-diagonal as well. □

3 Approximation and numerical results

Let us recall the variational formula obtained in Theorem 2.2,

$$F^{(\sigma)}(s) := \mathbb{P}\left(\max_{u\in\mathbb{R}}\left[\sqrt{2}\sigma B(u) + \mathcal{A}_2(u) - u^2\right] \le s\right). \tag{3.1}$$

While this defines the limit distribution, it seems to be difficult to either deduce more explicit expressions or to run numerical evaluations. To visualize our result we therefore return to the TASEP. The TASEP is particularly convenient as it is accessible by Monte Carlo simulations.

The TASEP exhibits well-known finite-time corrections. In particular, although the shape of the distribution is accurate even for relatively small times, one generically observes a shift, which is due to the slow $t^{-1/3}$ convergence of the first moment [23, 48, 49, 51]. The speed of convergence of the variance is $t^{-2/3}$. Therefore, in order to minimize the errors due to finite-time corrections, we extrapolate numerically the large time first and second cumulants and scale the numerical data to match the limiting first two cumulants. This procedure gives good results for the special case $\sigma = 0$ and $\sigma = 1$ for which the cumulants are known analytically as well.

Below we first present an approximate form of (3.1), which is then compared to Monte Carlo results. After that, we present a plot for the distribution (3.1) for several values of σ as well as a table with the numerically estimated cumulants. The latter might be useful for analyzing experimental results.

3.1 Approximate distribution for large σ

For large values of σ, the fluctuations of the initial Brownian motion should be more important than those from the Airy$_2$ process. A first approximation to (3.1) is to replace the $\mathcal{A}_2(u)$ just by $\mathcal{A}_2(0)$. In this case, the distribution function can be computed analytically. Indeed,

$$F^{(\sigma)}_{\rm appr}(s) := \mathbb{P}\left(\mathcal{A}_2(0) + \max_{u\in\mathbb{R}}\left[\sqrt{2}\sigma B(u) - u^2\right] \le s\right) \tag{3.2}$$

Since $\mathcal{A}_2(0)$ and $\max_{u\in\mathbb{R}}\left[\sqrt{2}\sigma B(u) - u^2\right]$ are independent random variables, $F^{(\sigma)}_{\rm appr}$ is the convolution of their distributions. We know that $\mathbb{P}(\mathcal{A}_2(0) \le s) = F_{\rm GUE}(s)$. The distribution function for $\max_{u\in\mathbb{R}}\left[\sqrt{2}\sigma B(u) - u^2\right]$ has been derived by Groeneboom [30], see also his more recent paper [31] describing a numerical evaluation. We denote by $F_{{\rm Gr},c}$ to be the Groeneboom distribution defined by

$$F_{{\rm Gr},c}(s) := \mathbb{P}\left(\max_{v\in\mathbb{R}}\left[B(v) - cv^2\right] \le s\right). \tag{3.3}$$

Then,

$$\mathbb{P}\left(\max_{u\in\mathbb{R}}\left[\sqrt{2}\sigma B(u) - u^2\right] \le s\right) = F_{{\rm Gr},1/\sqrt{2}}\left(\frac{s}{\sqrt{2}\sigma^{4/3}}\right) =: F^{(\sigma)}_{\rm Gr}(s). \tag{3.4}$$

As a consequence

$$F^{(\sigma)}_{\rm appr}(s) = \int_{\mathbb{R}} dx F'_{\rm GUE}(x) F^{(\sigma)}_{\rm Gr}(s-x). \tag{3.5}$$

The approximation $F^{(\sigma)}_{\rm appr}(s)$ of $F^{(\sigma)}(s)$ will not be very accurate for small values of s, since these corresponds to the realizations of B and $\mathcal{A}_2$ which are small around $u = 0$, and in that case asking that only B is small is not quite the same as B and $\mathcal{A}_2$ small. However, for larger values of s, the approximation should improve,

because the events leading to large maximums are due to large values of B and $\mathcal{A}_2$. Since $\mathcal{A}_2$ is stationary, these events should be dominated by large fluctuations of the Brownian motion.

A simplifying feature is that $F_{\text{appr}}^{(\sigma)}$ is the distribution of a sum of two independent random variables, their cumulants are just the sums of their cumulants. Furthermore, if we denote by $\kappa^{(n)}$, the nth cumulant of $F_{\text{Gr},1/\sqrt{2}}$, then the nth cumulant of $F_{\text{Gr}}^{(\sigma)}$ is given by $2^{n/2}\sigma^{4n/3}\kappa^{(n)}$.

The relevant cumulants are reported in Table 1.

Distribution	Mean	Variance	3rd cumulant	4th cumulant
F_{GUE}	-1.77108	0.8132	0.164	0.109
$F^{(0)} = \tilde{F}_{\text{GOE}}$	-0.76007	0.6381	0.149	0.067
$F^{(1)} = F_{\text{BR}}$	0	1.1504	0.444	0.383
$F_{\text{Gr},1/\sqrt{2}}$	0.8875	0.2646	0.128	0.080

Table 1: Table of the first four cumulants for a few distributions. Here $\tilde{F}_{\text{GOE}}(s) = F_{\text{GOE}}(2^{2/3}s)$.

3.2 Numerical comparison between $F_{\text{appr}}^{(\sigma)}$ and $F^{(\sigma)}$

After running TASEP simulations for a few values of σ, surprisingly the probability density plots of $F_{\text{appr}}^{(\sigma)}$ and $F^{(\sigma)}$ are already quite close even for fairly small values of σ. In Figures 3 and 4 we plot the probability densities of $F^{(\sigma)}(s)$ obtained from TASEP simulations and the approximation $F_{\text{appr}}^{(\sigma)}(s)$. In order to obtain the probability density of $F_{\text{appr}}^{(\sigma)}(s)$, we first use the formula of [31] to derive a table of values for the density of the Groeneboom distribution $F_{\text{Gr},1/\sqrt{2}}$ with values in $[0, 20]$ taking values every 10^{-3}, and then we numerically compute the convolution of the rescaled Groeneboom density with the GUE density.

3.3 Probability densities and cumulants for the entire range of σ

We report in Table 2 the cumulants obtained by the numerical simulation of TASEP. The values for $\sigma = 0$ and $\sigma = 1$ are known and they give an indication of the precision of the numerical simulation.

In Figure 5, the cumulants as a function of σ are illustrated, together with an empirical interpolation function (which is by no means to be thought of as an exact formula).

In Figure 6, we show the probability densities obtained by the Monte Carlo simulation for a subset of values of the α given in Table 2.

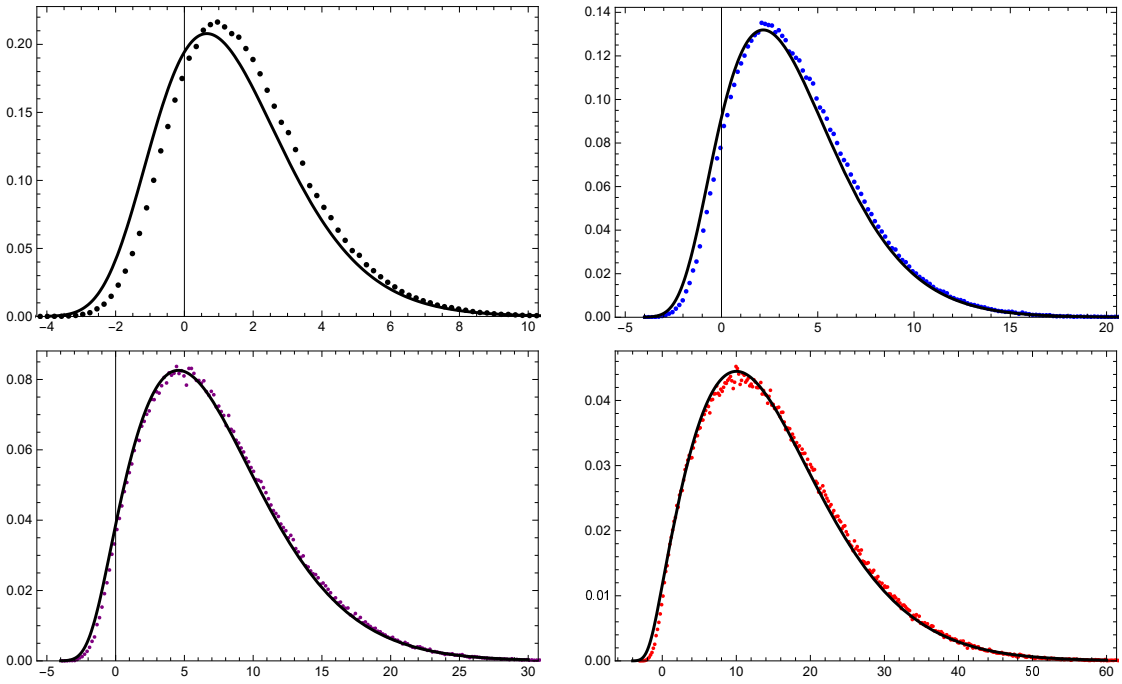

Figure 3: Comparison between the probability densities of $F^{(\sigma)}(s)$ and $F^{(\sigma)}_{\mathrm{appr}}(s)$: top-left is $\sigma = 2.0$, top-right is $\sigma = 3.0$, bottom-left is $\sigma = 4.36$ and bottom-right is $\sigma = 7.0$. The simulation for $\sigma = 2.0$ uses maximal time $t_{\max} = 2000$, while the other $t_{\max} = 3000$. The number of runs are 5×10^5 for each case.

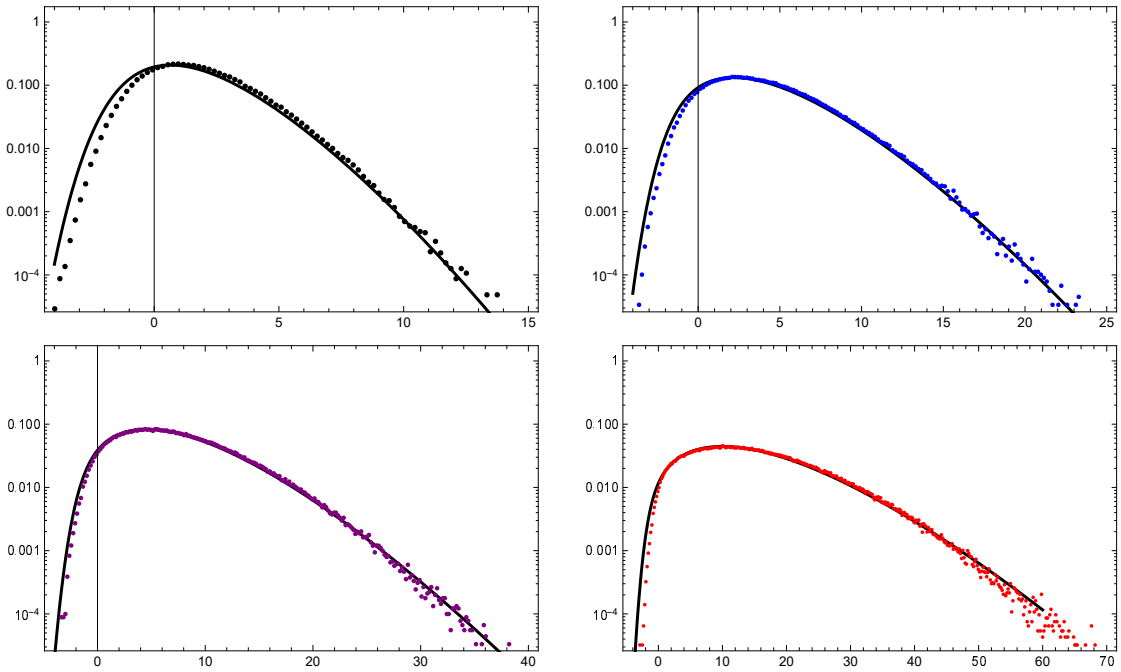

Figure 4: Logarithmic plots of the probability densities of Figure 3.

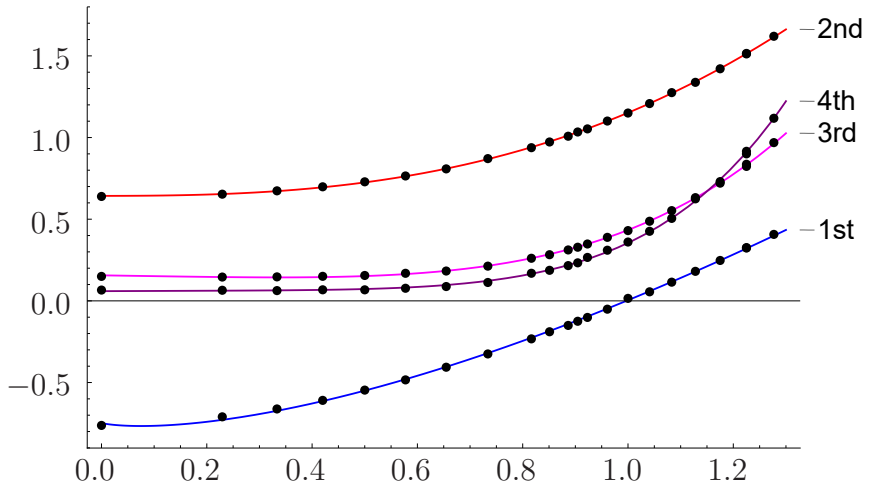

Figure 5: Empirical values for the first four cumulants of $F^{(\sigma)}$ as a function of σ. The empirical extrapolations are: $\kappa_1(\sigma) = -0.74795 - 0.96976\sigma + 1.7217\sigma^{4/3}$, $\kappa_2(\sigma) = 0.64268 + 0.0068163\sigma + 0.50202\sigma^{8/3}$, $\kappa_3(\sigma) = 0.15631 - 0.049956\sigma + 0.32731\sigma^4$, and $\kappa_4(\sigma) = 0.059476 + 0.012039\sigma + 0.28315\sigma^{16/3}$. The fitting made for the values shown in the figure, gives quite good results also for large values of σ

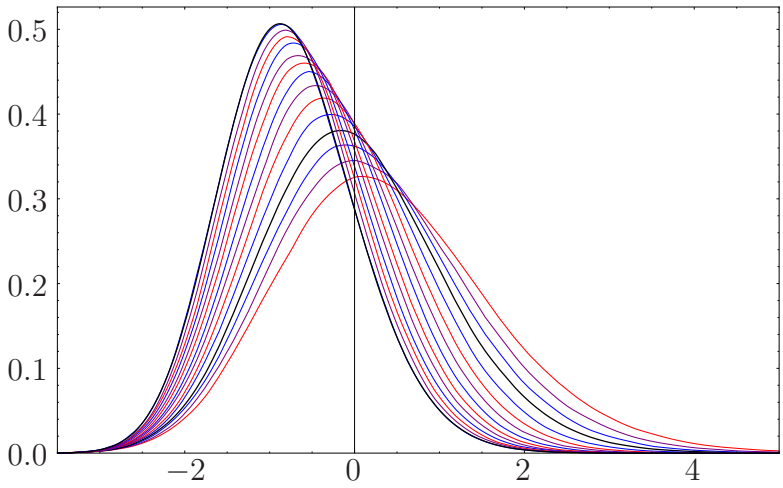

Figure 6: Probability densities of $F^{(\sigma)}(s)$ with $\sigma = \sqrt{\alpha/(1-\alpha)}$ from TASEP simulation until time $t_{\max} = 10^3$ and 10^6 runs. The different plots corresponds to the values $\alpha = 0, 0.05, 0.1, 0.15, 0.20, 0.25, 0.3, 0.35, 0.4, 0.45, 0.5, 0.54, 0.58, 0.62$. The left-most black line is the exact rescaled GOE distribution ($\sigma = 0$), which overlaps with $\alpha = 0$ from the simulations. The black line in the middle is the stationary case ($\sigma = 1$).

α	σ	Mean	Variance	3rd cumulant	4th cumulant
0	**0**	**-0.760**	**0.638**	**0.149**	**0.067**
0	0	-0.763	0.639	0.150	0.066
0.05	0.229	-0.710	0.653	0.146	0.065
0.10	0.333	-0.662	0.674	0.147	0.063
0.15	0.42	-0.609	0.698	0.15	0.068
0.20	0.5	-0.546	0.729	0.156	0.068
0.25	0.577	-0.484	0.765	0.169	0.077
0.30	0.655	-0.406	0.808	0.183	0.088
0.35	0.734	-0.325	0.871	0.213	0.11
0.40	0.816	-0.233	0.938	0.261	0.17
0.42	0.851	-0.189	0.973	0.283	0.19
0.44	0.886	-0.15	1.01	0.312	0.22
0.45	0.905	-0.125	1.03	0.328	0.23
0.46	0.923	-0.101	1.05	0.348	0.27
0.48	0.961	-0.051	1.10	0.389	0.31
0.5	**1**	**0**	**1.150**	**0.444**	**0.383**
0.50	1	0.002	1.15	0.430	0.36
0.52	1.04	0.056	1.21	0.487	0.43
0.54	1.08	0.115	1.27	0.552	0.51
0.56	1.13	0.181	1.34	0.632	0.63
0.58	1.18	0.247	1.42	0.721	0.73
0.60	1.22	0.326	1.51	0.836	0.92
0.62	1.28	0.407	1.62	0.969	1.1
0.64	1.33	0.494	1.73	1.12	1.3
0.70	1.53	0.822	2.23	1.87	2.7
0.80	2	1.72	3.93	5.49	11.7
0.90	3	3.91	10.5	28.1	102

Table 2: Table of cumulants obtained numerically by extrapolating the data. The bold numbers are the exactly known numbers. The higher the degree of the cumulant, the lower is the reliability on the numerical extrapolation.

4 The semi-infinite six-vertex model at its conical (KPZ) point

The planar six-vertex model can be viewed as a statistical mechanics model of interacting up-right lattice paths. Paths may touch, but they do not cross. The weight of such a collection of paths is defined by the product of the local weights, which in the canonical labeling are given by

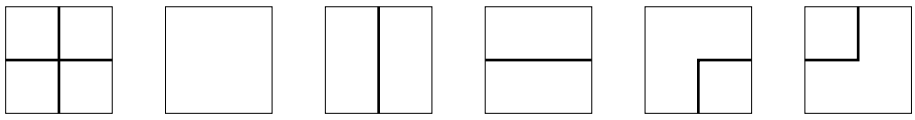

ω_1 ω_2 ω_3 ω_4 ω_5 ω_6

Much studied is the infinite volume limit with periodic boundary conditions. This results in a translation-invariant Gibbs measure, which might not be extremal, thereby possibly allowing for either ferro- or anti-ferroelectric ordering. A second popular choice are domain wall boundary conditions. For a given lattice square, all paths enter at the left edge and exit at the upper edge. There are no paths at the right and lower edge. If paths are interpreted as level lines of a surface over the two-dimensional lattice, then domain wall boundary conditions correspond to a surface boundary which varies on the macroscopic scale. Thus an arctic circle phenomenon is expected [17–19]. In fact, on its free fermion line the six-vertex model with domain wall boundary conditions is equivalent to the domino tiling of a lattice square rotated by $\pi/4$ [25], also known as Aztec diamond, which is well-studied [33, 36, 54].

In our context, the natural geometry is a semi-infinite lattice. For Ising type models, the influence of boundary fields have been widely studied [28], in particular close to criticality. We are not aware of corresponding investigations for the six-vertex model. So far, the results to be described hold only on the stochastic line, which is defined by

$$\vec{\omega} = (1, 1, q, p, 1-q, 1-p), \quad 0 \le p, q \le 1. \tag{4.1}$$

This choice is known as the conical point of the six-vertex model [15]. The name has its origin from studying the free energy, which depends on $\vec{\omega}$ only through four independent parameters. Using the anti-ferroelectric picture one fixes two temperature-like parameters with $\Delta > 1$ and considers the free energy as a function of the horizontal and vertical electric fields. The free energy has exactly two points satisfying (4.1) and a conical tip close to such point. The Gibbs measure at the tip exhibits KPZ type fluctuations.

The semi-infinite lattice is obtained by cutting along the anti-diagonal at which boundary conditions are imposed. The Gibbs measure of the semi-infinite lattice is then obtained through the diagonal transfer matrix, which in fact is a Markov chain. We introduce the occupation variables $\eta_{j,t} \in \{0, 1\}$, with 0 in case there is no path at the edge and 1 in case a path is crossing the edge. We use $j \in \mathbb{Z}$ as the spatial index and $t \in \mathbb{Z}$ as the temporal index. At two neighboring sites, $j, j+1$, the allowed states are $00, 10, 01, 11$. They are updated according to the transition matrix

$$T^{j,j+1} = \begin{pmatrix} 1 & 0 & 0 & 0 \\ 0 & 1-p & p & 0 \\ 0 & q & 1-q & 0 \\ 0 & 0 & 0 & 1 \end{pmatrix}. \tag{4.2}$$

The updates of the evenly blocked lattice, ...(01)(23)..., and the oddly blocked lattice, ...(12)(34)..., are alternate. Thus, the two step transition probability, T, is defined by

$$T = T_{\rm e}T_{\rm o}, \quad T_{\rm e} = \bigotimes_{j\in\mathbb{Z}} T^{2j,2j+1}, \quad T_{\rm o} = \bigotimes_{j\in\mathbb{Z}} T^{2j-1,2j}, \tag{4.3}$$

all acting on $\{0,1\}^{\mathbb{Z}}$.

Let us consider the alternating product measure $\mu_{(a,b)} = ... \otimes \mu_{\rm e} \otimes \mu_{\rm o} \otimes ...$, setting $\mu_{\rm e}(1) = a$, $\mu_{\rm o}(1) = b$ (say with $\mu_{\rm e}$ on even and $\mu_{\rm o}$ on odd sites). If

$$(1-q)(1-b)a = (1-p)b(1-a), \tag{4.4}$$

then, denoting by τ the lattice shift,

$$\mu_{(a,b)}T_* = \mu_{(a,b)} \circ \tau, \text{ with } * \in \{{\rm e},{\rm o}\}. \tag{4.5}$$

Hence T has a one-parameter family of stationary measures $\mu_{(a^*,b^*)}$, a^*, b^* solution of (4.4). Thereby we arrive at the Markov chain $\eta_{j,t}$, stationary in both j and t. By construction, this is an extremal Gibbs measure of the six-vertex model with vertex weights (4.1). An alternative construction is explained in [1]. The density-current relation, $\mathsf{j}(\rho)$, of this process is the solution to

$$\mathsf{j}^2 + ((2-p-q)/(q-p))\mathsf{j} + \rho(1-\rho) = 0. \tag{4.6}$$

Small perturbations travel with velocity $v = \mathsf{j}'(\rho)$. The two-point function $S(j,t) = \mathbb{E}(\eta_{j,t}\eta_{0,0}) - \mathbb{E}(\eta_{j,t})\mathbb{E}(\eta_{0,0})$, decays exponentially except along the special line $\{j = vt\}$. At distance of order $t^{2/3}$ to this line, according to KPZ scaling theory [38] (we use the normalisation as in (12) of [50]) one has the scaling form

$$S(j,t) \simeq A(\Gamma t)^{-2/3} f_{\rm KPZ}\big((\Gamma t)^{-2/3}(j-vt)\big) \tag{4.7}$$

with $\Gamma = \frac{1}{2}A^2|\mathsf{j}''(\rho)|$, where A is the wandering coefficient in the stationary case. In particular, $S(j,t)$ decays as $t^{-2/3}$ along $\{j = vt\}$.

If the boundary field $\eta_{j,0}$ satisfies a central limit theorem as in (2.6), then our theory predicts a scaling behavior identical to (4.7), except that $f_{\rm KPZ}$ has to be replaced by a different scaling function. In fact, at stationarity, this scaling function is related to the variance of the random variable on the right hand side of (2.9), see Proposition 4.1 in [42].

To test our predictions, we consider the boundary fields $\mu_{(a,b)}$ with general $0 \le a, b \le 1$. Then Assumption 2.1 holds with

$$\sigma^2 = \tfrac{1}{4\gamma}\big(a(1-a) + b(1-b)\big) \quad \text{and} \quad \gamma = \tfrac{1}{4}\left(a^*(1-a^*) + b^*(1-b^*)\right). \tag{4.8}$$

For the simulation we set $\mathbb{E}(\eta_{j,0}) + \mathbb{E}(\eta_{j+1,0}) = 2\rho = 1$, which implies $v = 0$ and $a + b = 1$ and thus $\sigma^2 = a(1-a)/(2\gamma)$. In addition imposing stationarity, the unique solution of (4.4) in $[0,1]$ is $a = a^* = a_{\rm BR}$ given by

$$a_{\rm BR} = \frac{1-q-\sqrt{(1-p)(1-q)}}{p-q}. \tag{4.9}$$

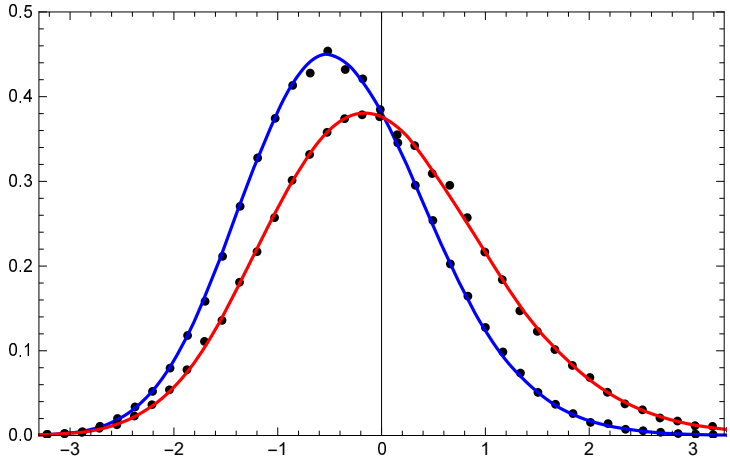

Figure 7: Illustration of the universality: for $\sigma^2 = \alpha/(1-\alpha)$ with $\alpha = 0.3$ (blue) and the stationary benchmark $\alpha = 0.5$ (red), the dots are the probabilities for the current fluctuations of the stochastic six-vertex model. Here we choose generic values, $p = 0.6$, $q = 0.2$, and particle density $\rho = 1/2$. The data are scaled according to KPZ scaling theory. We also considered the first order correction (known to generically decay as $t^{-1/3}$ [23,48,49,51]), which however resulted only in minimal shifts (0.011 resp. 0.005). The solid line is the result of TASEP simulation for the same value of σ. The number of Monte Carlo runs is 10^5.

Let us denote by $J(t)$ the current at the origin summed over the time span $[0,t]$. At density $\rho = 1/2$, for the scaling coefficient Γ we have to set $a = a_{\mathrm{BR}}$ and a computation gives $|\mathsf{j}''(\rho)| = |p-q|/\sqrt{(1-p)(1-q)}$. The stationary current is given by $\mathsf{j} = a_{\mathrm{BR}}(1-a_{\mathrm{BR}})(p-q)/2 = a_{\mathrm{BR}} - 1/2$. Thus, by the KPZ scaling theory, we expect that

$$\lim_{t\to\infty} \mathbb{P}\left(\frac{J(t) - \mathsf{j}t}{-(\Gamma t)^{1/3}} \le s\right) = F^{(\sigma)}(s), \tag{4.10}$$

where the values of a and b for generic σ are

$$a = \tfrac{1}{2}(1 - \sqrt{1 - 4\sigma^2 a_{\mathrm{BR}}(1-a_{\mathrm{BR}})}), \quad b = 1 - a = \tfrac{1}{2}(1 + \sqrt{1 - 4\sigma^2 a_{\mathrm{BR}}(1-a_{\mathrm{BR}})}), \tag{4.11}$$

since (4.8) has to be satisfied and for $\sigma = 1$ also (4.4). By varying a, we realize the family of universal distributions $F^{(\sigma)}$ with $\sigma \in [0, \sigma_{\max}]$, where $\sigma^2_{\max} = (4a_{\mathrm{BR}}(1-a_{\mathrm{BR}}))^{-1} > 1$. The theoretical prediction (4.10) is checked for a generic value of (p,q) and two values of the diffusion coefficient σ, namely $\sigma^2 = 3/7$ and the stationary case. The numerical agreement is very precise as illustrated in Figures 7 and 8.

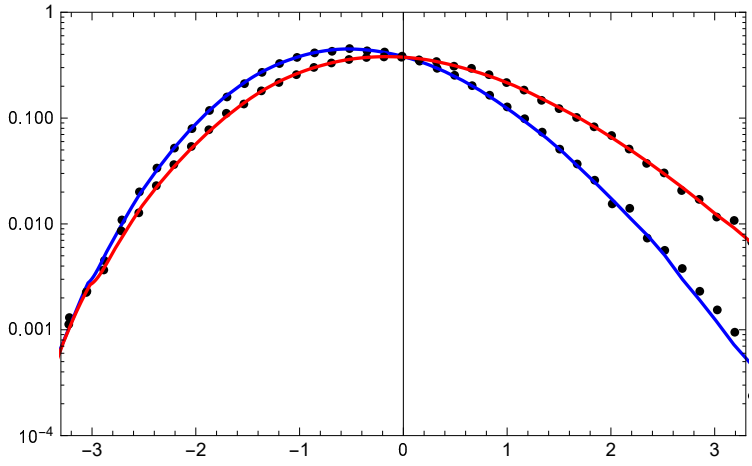

Figure 8: Logarithmic plot of the probability densities of Figure 7.

References

[1] A. Aggarwal, *Current Fluctuations of the Stationary ASEP and Six-Vertex Model*, arXiv:1608.04726 (2016).

[2] G. Amir, I. Corwin, and J. Quastel, *Probability distribution of the free energy of the continuum directed random polymer in 1+1 dimensions*, Comm. Pure Appl. Math. **64** (2011), 466–537.

[3] J. Baik, G. Ben Arous, and S. Péché, *Phase transition of the largest eigenvalue for non-null complex sample covariance matrices*, Ann. Probab. **33** (2006), 1643–1697.

[4] J. Baik, P.A. Deift, and K. Johansson, *On the distribution of the length of the longest increasing subsequence of random permutations*, J. Amer. Math. Soc. **12** (1999), 1119–1178.

[5] J. Baik, P.L. Ferrari, and S. Péché, *Limit process of stationary TASEP near the characteristic line*, Comm. Pure Appl. Math. **63** (2010), 1017–1070.

[6] J. Baik, P.L. Ferrari, and S. Péché, *Convergence of the two-point function of the stationary TASEP*, Singular Phenomena and Scaling in Mathematical Models, Springer, 2014, pp. 91–110.

[7] J. Baik and E.M. Rains, *Limiting distributions for a polynuclear growth model with external sources*, J. Stat. Phys. **100** (2000), 523–542.

[8] J. Baik and E.M. Rains, *Symmetrized random permutations*, Random Matrix Models and Their Applications, vol. 40, Cambridge University Press, 2001, pp. 1–19.

[9] P. Billingsley, *Convergence of Probability Measures*, Wiley ed., New York, 1968.

[10] A. Borodin, I. Corwin, P.L. Ferrari, and B. Vető, *Height fluctuations for the stationary KPZ equation*, Math. Phys. Anal. Geom. **18:20** (2015).

[11] A. Borodin, I. Corwin, and V. Gorin, *Stochastic six-vertex model*, Duke Math. J. **165** (2016), 563–624.

[12] A. Borodin, P.L. Ferrari, M. Prähofer, and T. Sasamoto, *Fluctuation properties of the TASEP with periodic initial configuration*, J. Stat. Phys. **129** (2007), 1055–1080.

[13] A. Borodin, P.L. Ferrari, and T. Sasamoto, *Transition between $Airy_1$ and $Airy_2$ processes and TASEP fluctuations*, Comm. Pure Appl. Math. **61** (2008), 1603–1629.

[14] A. Borodin and S. Péché, *Airy Kernel with Two Sets of Parameters in Directed Percolation and Random Matrix Theory*, J. Stat. Phys. **132** (2008), 275–290.

[15] D.J. Bukman and J.D. Shore, *The conical point in the ferroelectric six-vertex model*, J. Stat. Phys. **78** (1995), 1277–1309.

[16] E. Cator and L. Pimentel, *On the local fluctuations of last-passage percolation models*, Stoch. Proc. Appl. **125** (2015), 879–903.

[17] F. Colomo and A. Pronko, *Third-order phase transition in random tilings*, Phys. Rev. E **88** (2013), 042125.

[18] F. Colomo and A. Pronko, *Thermodynamics of the six-vertex model in an L-shaped domain*, Comm. Math. Phys. **339** (2015), 699–728.

[19] F. Colomo and A. Sportiello, *Arctic curves of the six-vertex model on generic domains: the Tangent Method*, arXiv:1605.01388 (2016).

[20] I. Corwin, P.L. Ferrari, and S. Péché, *Universality of slow decorrelation in KPZ models*, Ann. Inst. H. Poincaré Probab. Statist. **48** (2012), 134–150.

[21] I. Corwin and A. Hammond, *Brownian Gibbs property for Airy line ensembles*, Inventiones mathematicae **195** (2013), 441–508.

[22] I. Corwin, Z. Liu, and D. Wang, *Fluctuations of TASEP and LPP with general initial data*, Ann. Appl. Probab. **26** (2016), 2030–2082.

[23] P.L. Ferrari and R. Frings, *Finite time corrections in KPZ growth models*, J. Stat. Phys. **144** (2011), 1123–1150.

[24] P.L. Ferrari and P. Nejjar, *Anomalous shock fluctuations in TASEP and last passage percolation models*, Probab. Theory Relat. Fields **161** (2015), 61–109.

[25] P.L. Ferrari and H. Spohn, *Domino tilings and the six-vertex model at its free fermion point*, J. Phys. A: Math. Gen. **39** (2006), 10297–10306.

[26] P.L. Ferrari and H. Spohn, *Scaling limit for the space-time covariance of the stationary totally asymmetric simple exclusion process*, Comm. Math. Phys. **265** (2006), 1–44.

[27] P.L. Ferrari and B. Vető, *Tracy-Widom asymptotics for q-TASEP*, Ann. Inst. H. Poincaré, Probab. Statist. **51** (2015), 1465–1485.

[28] J. Fröhlich and C. Pfister, *Semi-infinite Ising model, I. Thermodynamic functions and phase diagram in absence of magnetic field*, Comm. Math. Phys. **109** (1987), 493–523.

[29] P. Groeneboom, *Estimating a monotone density*, Proceedings of the Berkeley Conference in Honor of Jerzy Neyman and Jack Kiefer, II (L.M. Le Cam and R.A. Olshen, eds.), 1985, pp. 535–555.

[30] P. Groeneboom, *Brownian motion with a parabolic drift and Airy functions*, Probab. Theory Related Fields **81** (1989), 79–109.

[31] P. Groeneboom, *The maximum of Brownian motion minus a parabola*, Electron. J. Probab. **15** (2010), 1930–1937.

[32] T. Imamura and T. Sasamoto, *Polynuclear growth model with external source and random matrix model with deterministic source*, Phys. Rev. E **71** (2005), 041606.

[33] W. Jockush, J. Propp, and P. Shor, *Random domino tilings and the arctic circle theorem*, arXiv:math.CO/9801068 (1998).

[34] K. Johansson, *Shape fluctuations and random matrices*, Comm. Math. Phys. **209** (2000), 437–476.

[35] K. Johansson, *Discrete polynuclear growth and determinantal processes*, Comm. Math. Phys. **242** (2003), 277–329.

[36] K. Johansson, *The arctic circle boundary and the Airy process*, Ann. Probab. **33** (2005), 1–30.

[37] C. Kipnis and S.R.S. Varadhan, *Central limit theorem for additive functionals of reversible Markov processes and applications to simple exclusions*, Comm. Math. Phys. **104** (1986), 1–19.

[38] J. Krug, P. Meakin, and T. Halpin-Healy, *Amplitude universality for driven interfaces and directed polymers in random media*, Phys. Rev. A **45** (1992), 638–653.

[39] T.M. Liggett, *Coupling the simple exclusion process*, Ann. Probab. **4** (1976), 339–356.

[40] T.M. Liggett, *Stochastic interacting systems: contact, voter and exclusion processes*, Springer Verlag, Berlin, 1999.

[41] M. Prähofer and H. Spohn, *Universal distributions for growth processes in 1+1 dimensions and random matrices*, Phys. Rev. Lett. **84** (2000), 4882–4885.

[42] M. Prähofer and H. Spohn, *Current fluctuations for the totally asymmetric simple exclusion process*, In and out of equilibrium (V. Sidoravicius, ed.), Progress in Probability, Birkhäuser, 2002.

[43] M. Prähofer and H. Spohn, *Scale invariance of the PNG droplet and the Airy process*, J. Stat. Phys. **108** (2002), 1071–1106.

[44] J. Quastel and D. Remenik, *How flat is flat in a random interface growth?*, arXiv:1606.09228 (2016).

[45] T. Sasamoto, *Fluctuations of the one-dimensional asymmetric exclusion process using random matrix techniques*, J. Stat. Mech. **P07007** (2007).

[46] T. Sasamoto and H. Spohn, *The crossover regime for the weakly asymmetric simple exclusion process*, J. Stat. Phys. **140** (2010), 209–231.

[47] D. Szász and B. Tóth, *Persistent random walks in a one-dimensional random environment*, J. Stat. Phys. **37** (1984), 27–38.

[48] K.A. Takeuchi, *Statistics of circular interface fluctuations in an off-lattice Eden model*, J. Stat. Mech. (2012), P05007.

[49] K.A. Takeuchi and M. Sano, *Growing interfaces of liquid crystal turbulence: universal scaling and fluctuations*, Phys. Rev. Lett. **104** (2010), 230601.

[50] K.A. Takeuchi and M. Sano, *Evidence for geometry-dependent universal fluctuations of the Kardar-Parisi-Zhang interfaces in liquid-crystal turbulence*, J. Stat. Phys. **147** (2012), 853–890.

[51] K.A. Takeuchi, M. Sano, T. Sasamoto, and H. Spohn, *Growing interfaces uncover universal fluctuations behind scale invariance*, Sci. Rep. **1** (2011), 34.

[52] C.A. Tracy and H. Widom, *Level-spacing distributions and the Airy kernel*, Comm. Math. Phys. **159** (1994), 151–174.

[53] C.A. Tracy and H. Widom, *On orthogonal and symplectic matrix ensembles*, Comm. Math. Phys. **177** (1996), 727–754.

[54] P. Zinn-Justin, *Six-vertex model with domain wall boundary conditions and one-matrix models*, Phys. Rev. E **62** (2000), 3411–3418.